Available online at www.sciencedirect.com
ScienceDirect
Ore Geology Reviews 32 (2007) 471–499
ORE GEOLOGY REVIEWS
www.elsevier.com/locate/oregeorev

Lithofacies associations and structural evolution of the Archean Rio das Velhas greenstone belt, Quadrilátero Ferrífero, Brazil: A review of the setting of gold deposits

O.F. Baltazar *, M. Zucchetti

CPRM–Geological Survey of Brazil, Av. Brasil 1731, Funcionários, Belo Horizonte, Minas Gerais, 30140-002, Brazil

Received 10 April 2003; accepted 29 March 2005
Available online 6 March 2007

Abstract

The Rio das Velhas greenstone belt is located in the Quadrilátero Ferrífero region, in the southern extremity of the São Francisco Craton, central-southern part of the State of Minas Gerais, SE Brazil. The metavolcano–sedimentary rocks of the Rio das Velhas Supergroup in this region are subdivided into the Nova Lima and Maquiné Groups. The former occurs at the base of the sequence, and contains the major Au deposits of the region. New geochronological data, along with a review of geochemical data for volcanic and sedimentary rocks, suggest at least two generations of greenstone belts, dated at 2900 and 2780 Ma. Seven lithofacies associations are identified, from bottom to top, encompassing (1) mafic–ultramafic volcanic; (2) volcano–chemical–sedimentary; (3) clastic–chemical–sedimentary, (4) volcaniclastic association with four lithofacies: monomictic and polymictic breccias, conglomerate–graywacke, graywacke–sandstone, graywacke–argillite; (5) resedimented association, including three sequences of graywacke–argillite, in the north and eastern, at greenschist facies and in the south, at amphibolite metamorphic facies; (6) coastal association with four lithofacies: sandstone with medium- to large-scale cross-bedding, sandstone with ripple marks, sandstone with herringbone cross-bedding, sandstone–siltstone; (7) non-marine association with the lithofacies: conglomerate–sandstone, coarse-grained sandstone, fine- to medium-grained sandstone. Four generations of structures are recognized: the first and second are Archean and compressional, driven from NNE to SSW; the third is extensional and attributed to the Paleoproterozoic Transamazonian Orogenic Cycle; and the fourth is compressional, driven from E to W, is related to the Neoproterozoic Brasiliano Orogenic Cycle. Gold deposits in the Rio das Velhas greenstone belt are structurally controlled and occur associated with hydrothermal alterations along Archean thrust shear zones of the second generation of structures.

Sedimentation occurred during four episodes. Cycle 1 is interpreted to have occurred between 2800 and 2780 Ma, based on the ages of the mafic and felsic volcanism, and comprises predominantly chemical sedimentary rocks intercalated with mafic–ultramafic volcanic flows. It includes the volcano–chemical–sedimentary lithofacies association and part of the mafic–ultramafic volcanic association. The cycle is related to the initial extensional stage of the greenstone belt formation, with the deposition of sediments contemporaneous with volcanic flows that formed the submarine mafic plains. Cycle 2 encompasses the clastic–chemical–sedimentary association and distal turbidites of the resedimented association, in the eastern sector of the Quadrilátero Ferrífero. It was deposited in the initial stages of the felsic volcanism. Cycle 2 includes the coastal and resedimented associations in the southern sector, in advanced stages of subduction. In this southern sedimentary cycle it is also possible to recognize a stable shelf environment. Following the felsic volcanism, Cycle 3 comprises sedimentary rocks of the volcaniclastic and resedimented lithofacies associations, largely in the northern sector of the area. The characteristics of both associations indicate a submarine fan environment transitional to non-marine successions related to felsic volcanic edifices and related to the formation of island arcs.

* Corresponding author.
E-mail address: orivaldo@bh.cprm.gov.br (O.F. Baltazar).

doi:10.1016/j.oregeorev.2005.03.021

Cycle 4 is made up of clastic sedimentary rocks belonging to the non-marine lithofacies association. They are interpreted as braided plain and alluvial fan deposits in a retroarc foreland basin with the supply of debris from the previous cycles.

Keywords: Rio das Velhas greenstone belt; Archean; Lithofacies associations; Volcano–sedimentary cycle; Structural evolution

1. Introduction

The Quadrilátero Ferrífero region covers an area of about 700 km^2 of the southern part of the São Francisco Craton (Almeida, 1967; Almeida and Hasui, 1984), in the SE region of Brazil and the central-southern region of the State of Minas Gerais (Fig. 1). The Quadrilátero Ferrífero (QF) consists of three main units: Archean granite–gneiss terrains, Archean volcano–sedimentary sequences, including the Rio das Velhas greenstone belt, and Proterozoic sedimentary and volcano–sedimentary cover sequences. Dorr et al. (1957) included the meta-volcanic–sedimentary rocks of the QF into the Rio das Velhas Series, subsequently subdivided into the Nova Lima and Maquiné Groups (Dorr, 1969). The Nova Lima Group represents the basal volcano–sedimentary unit. In spite of its importance in terms of the world-class gold deposits it hosts (Lobato et al., 2001c), there have only been attempts at local stratigraphic subdivisions in areas of Au deposits. From 1992 to 1996, the Geological Survey of Brazil (CPRM) carried out geological mapping of the greenstone belt within the QF, at a scale of 1:25,000, subdividing the Nova Lima and Maquiné Groups into informal units (Baltazar and Silva, 1996; Zucchetti et al., 1996, 1998). This was based on the recognition of volcano–sedimentary and sedimentary lithofacies, their stratigraphic relationships, and their grouping into associations (Baltazar et al., 1995; Pedreira and Silva, 1996; Baltazar and Pedreira, 1996, 1998).

This paper reviews the geology of the Rio das Velhas greenstone belt, concentrating on stratigraphic and structural aspects, and providing a regional setting for the Au deposits described in other papers in this special issue. This review is based mainly on data obtained during 1:25,000 mapping, integrated with new field observations and the work of other authors carried out subsequent to the mapping. In this way, the known lithofacies associations were reviewed (Baltazar et al., 1994; Pedreira and Silva, 1996; Baltazar and Pedreira, 1996; Golia, 1997; Baltazar and Pedreira, 1998; Zucchetti and Baltazar, 2000; Zucchetti et al., 2000a) and new sedimentary lithofacies described. Together with the evaluation of the few isotopic ages available (Machado et al., 1989; Machado et al., 1992; Carneiro, 1992; Renger et al., 1994; Machado et al., 1996; Schrank and Machado, 1996a,b; Noce et al., 1998; Noce, 2000; Noce et al., 2002; Schrank et al., 2002; Suita et al., 2002), and a review of petrographic, geochemical and structural data, it is possible to produce a preliminary, paleoenvironmental interpretation of the Rio das Velhas greenstone belt. Comparisons are made with better known Archean greenstone belts in other parts of the world. Four sedimentation cycles are defined in time and space, with or without associated volcanism, as well as successive phases of deformation responsible for the current architecture of the greenstone belt. As a consequence, a new stratigraphic subdivision, based on the proposal of Baltazar and Silva (1996) and Zucchetti et al. (1996, 1998), is suggested. For greater clarity, the terminology of the original pre-metamorphic sedimentary rocks is used and stratigraphic names are avoided.

2. Geological setting

The QF covers: (1) an Archean to Proterozoic granite–gneiss terrain, (2) Archean greenstone belts, and (3) Proterozoic supracrustal sequences. The granite–gneiss terrain is made up of Archean trondhjemite–tonalite–granodiorite (TTG) gneisses (e.g., Belo Horizonte, Caeté, Santa Bárbara and Bação complexes) formed in the 3380 to 2900 Ma interval (Teixeira et al., 1996). Migmatization took place at $2860+14/-10$ Ma and 2772 ± 6 Ma, and Transamazonian metamorphic resetting took place at 2041 ± 5 Ma (Noce et al., 1998; U–Pb ages in zircon). Schrank and Machado (1996b) and Schrank et al. (2002) considered that the interval from 2920 to 2834 Ma corresponds to the last major episode of metamorphism/magmatism of the source area of detritus of the Rio das Velhas greenstone belt, and named it the Belo Horizonte Event.

The tonalite–trondhjemite–granodiorite gneisses (TTG) are intruded by Neoarchean and Paleoproterozoic granitoids. The Neoarchean granitoids are grouped into three episodes: 2780 to 2760 Ma, 2720 to 2.700 Ma and ~2600 Ma (Noce, 2000), based on U–Pb and Pb–Pb zircon dating. Widespread intrusion of granitoid bodies in the south of the QF occurred during the Paleoproterozoic in both the greenstone sequences and in ancient Archean

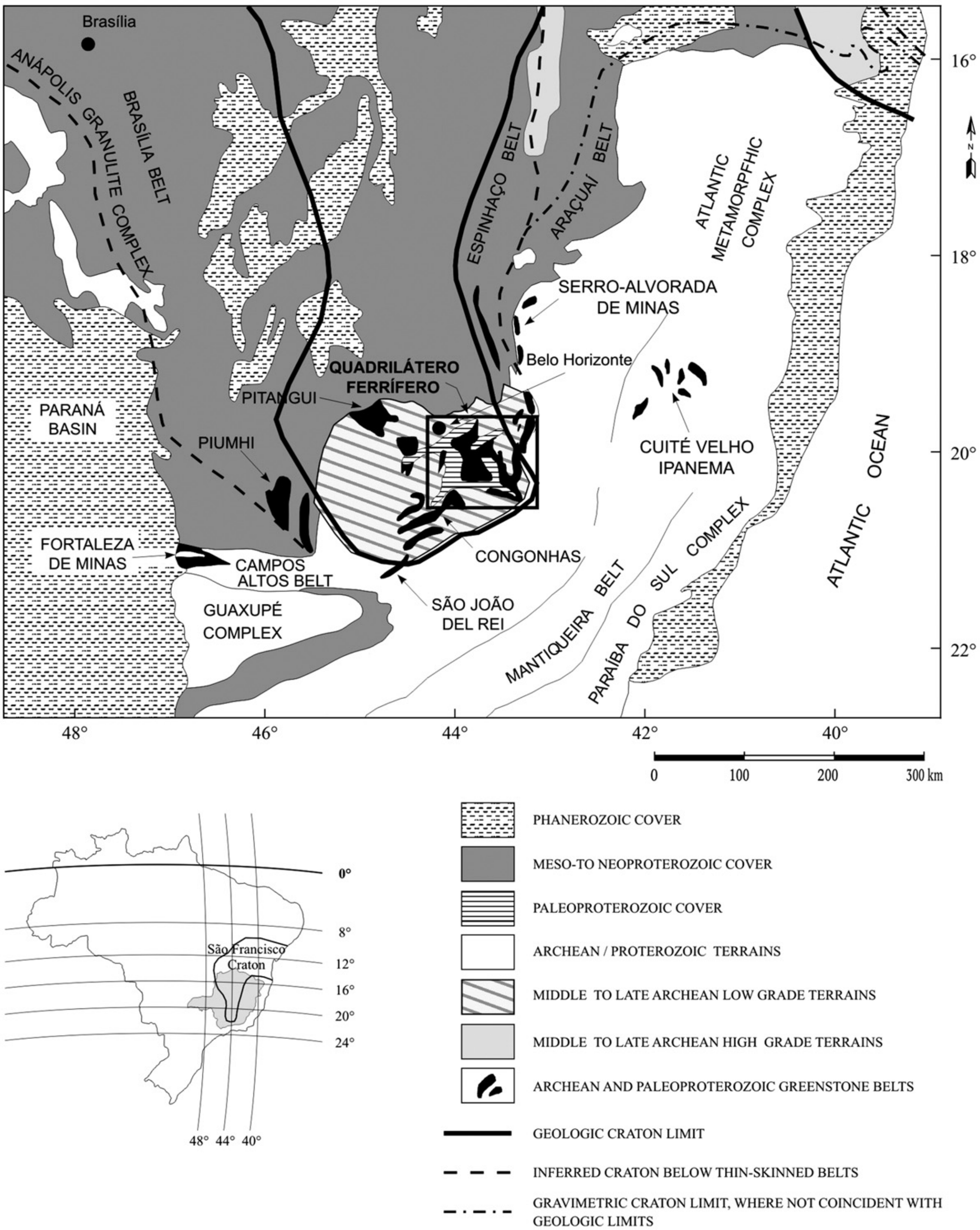

Fig. 1. Regional geological map of the southern São Francisco craton (modified after Lobato et al., 2001a). The Quadrilátero Ferrífero region, in the southernmost part of the craton, is indicated. Insert refers to Fig. 2.

crust. These tonalitic and granitic bodies make up the Mineiro Belt, which evolved during the Transamazonic Orogenetic Cycle (Teixeira, 1985; Carneiro, 1992; Noce et al., 1998), with isotopic ages of 2200 to 1900 Ma.

The Rio das Velhas greenstone belt comprises the Nova Lima and Maquiné Groups. The Nova Lima Group has: (1) a basal tholeiitic–komatiitic, volcanic unit with abundant associated chemical sedimentary rocks, (2) an overlying volcaniclastic unit, with associated felsic volcanism, and (3) an upper clastic unit. The age of basaltic volcanism is indicated to be 2927 ± 180 Ma by Sm–Nd whole-rock analyses (Lobato et al., 2001c). The felsic volcanism is dated at 3035 Ma (U–Pb zircon age; Machado et al., 1992; Noce et al.,

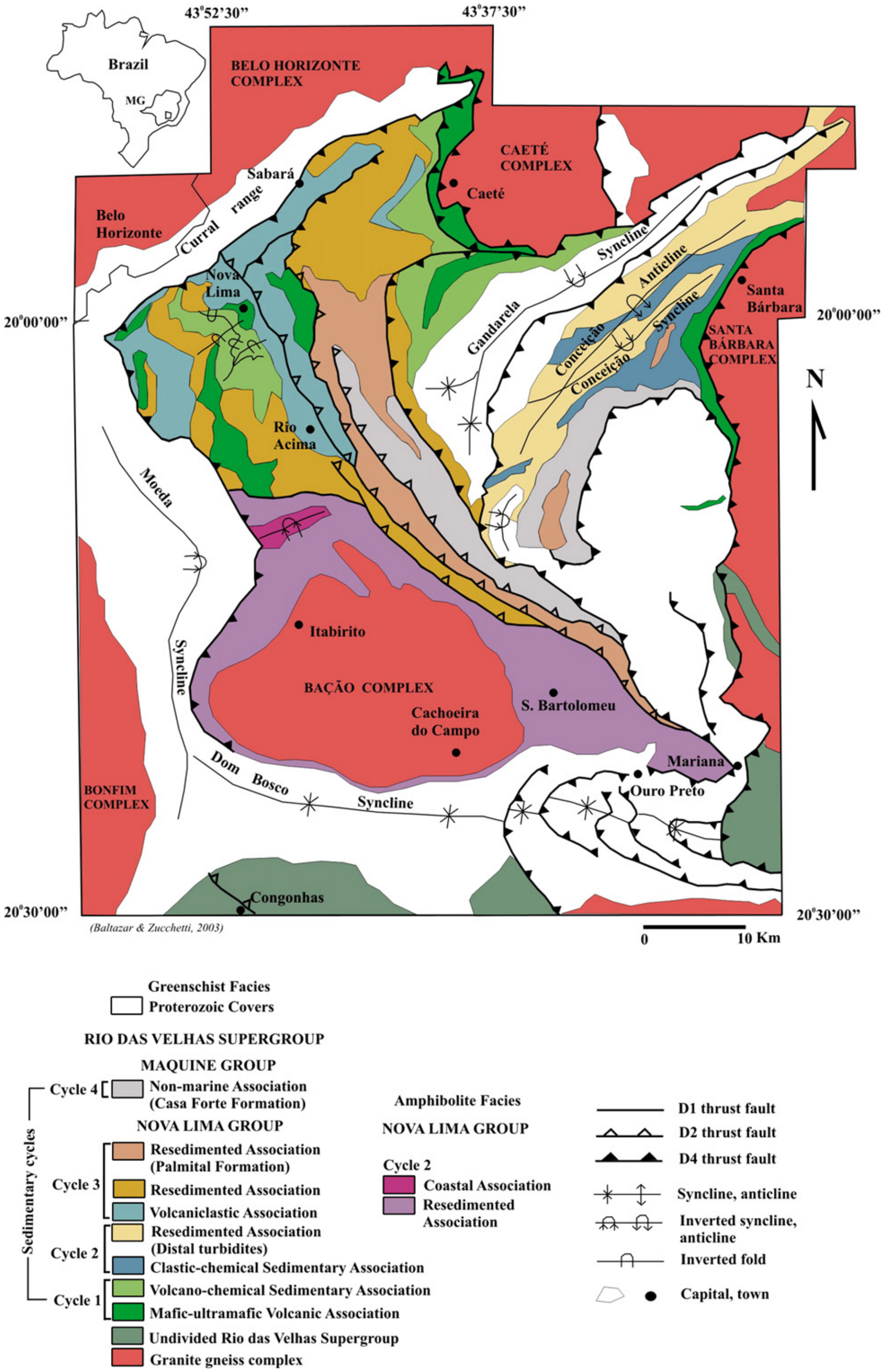

Fig. 2. Simplified geological map of the Rio das Velhas greenstone belt included in the Quadrilátero Ferrífero (modified after Zucchetti et al., 2000a).

2002); 2930 Ma (Pb–Pb zircon age; Noce et al., 2002); 2800 Ma (SHRIMP U–Pb zircon; Trendall, in Lobato et al., 2001b); and within the 2776–2772 Ma interval (U–Pb in zircon; Machado et al., 1992). This latter age is contemporaneous with the crystallization of the Caeté complex granodiorite (Fig. 2), dated at 2776 Ma (U–Pb zircon age; Machado et al., 1992). Carneiro (1992) named the 2.78 to 2.70 Ga interval the Rio das Velhas Orogenic Event, in which there was reworking of Archean sialic crust, intrusion of tonalitic bodies and felsic volcanism of the Rio das Velhas greenstone belt. The clastic sedimentary rocks of the upper unit of the greenstone belt are dominated by graywacke–argillite sequences, with evidence of significant contribution from both the felsic volcanic rocks of the greenstone belt and the reworked ancient Archean crust. The Maquiné Group sandstones and conglomerates overlie the Nova Lima Group along an angular unconformity.

The Proterozoic supercrustal sequences are made up of the Minas Supergroup (predominantly), Itacolomi Group and Espinhaço Supergroup. The distribution of the Minas Supergroup defines the geometrical shape of the QF, the limits of which are defined by synclinal megafolds (Fig. 2). The Minas Supergroup represents a continental margin sequence, with sedimentation age between 2580 and 2050 Ma (Renger et al., 1994), or between 2600 and 2125 Ma (LA-ICPMS Pb–Pb in zircon) according to Machado et al. (1996). The Minas Supergroup overlies the greenstone belt along an angular and erosive unconformity. The clastic sedimentary rocks of the Itacolomi Group, overlying the Minas Supergroup along an angular unconformity, contain zircons with a minimum age of about 2060 Ma (LA-ICPMS Pb–Pb in zircon; Machado et al., 1996). The Espinhaço Supergroup, which covers a small area in the QF, was deposited in the Paleoproterozoic, about 1840 to 1715 Ma (U–Pb; Machado et al., 1989).

Table 1
Stratigraphy of the Rio das Velhas greenstone belt inside the Quadrilátero Ferrífero (modified after Zucchetti and Baltazar, 1998)

		Nova Lima–Caeté block	S. Bárbara block	S. Bartolomeu block	Lithofacies associations (settings)	Cycle
Maquiné Group	Casa Forte Formation	Framework-supported conglomerate–sandstone, graded-bedded sandstone	Matrix-supported conglomerate-sandstone, fine- to medium-grained sandstone		Non-marine (alluvial fan, fluvial braided)	IV
Nova Lima Group	Palmital Formation	Graywacke–argillite, sandstone Graywacke–argillite; Bouma cycle			Resedimented (proximal turbidite) (Distal turbidites)	III
		Polymictic and monomictic breccia, conglomerate–graywacke, graywacke–sandstone, graywacke–argillite			Volcaniclastic (alluvial fan-fluvial; turbidite)	
				Ripple marks sandstone, herringbone cross-bedded sandstone, large-scale cross-bedded sandstone, sandstone–argillite	Coastal (tidal plain, aeolic dunes)	II
		Graywacke–argillite; Bouma cycle		Graywacke–argillite, calcissilicatic rock interbedded; Bouma cycles; minor polymictic conglomerate and BIF	Resedimented (marine–turbidites)	
			BIF, pelite, carbonaceous pelite		Clastic–chemical–sedimentary (pelagic sedimentary rocks)	
		BIF, chert, basalt; minor volcanic felsic rock, pelite and graywacke			Volcano–chemical–sedimentary (pelagic facies, submarine plateaus)	II
		Mg–basalt, tholeiitic basalt, minor komatiite, graywacke and BIF	Komatiite; minor tholeiitic basalt		Mafic–ultramafic volcanic (submarine plateaus)	

3. Stratigraphy

The main stratigraphic subdivisions proposed for the Rio das Velhas greenstone belt are those of Dorr et al. (1957), Dorr (1969), Ladeira (1980), Baltazar and Silva (1996) and Zucchetti et al. (1996, 1998). The Nova Lima Group comprises mainly basic lavas, graywacke and quartzite, with iron formation intercalations, quartz–dolomite and quartz–ankerite rocks ('lapa seca' — the host to the world-class Morro Velho gold deposit; Vial et al., 2007-this volume), conglomerates and carbonaceous phyllite. The Maquiné Group has been divided into the basal Palmital (O'Rourke, 1957) and Casa Forte (Gair, 1962) Formations, the former with quartzite and quartz–phyllite, and the latter with quartzite and conglomerate (Dorr, 1969). The Maquiné Group is interpreted to overlie the Nova Lima Group, in places both unconformably and conformably, and also along gradational contacts. The contacts of the volcano–sedimentary sequence with the granite–gneiss terrain are of intrusive or faulted nature. Almeida (1976) and Schorscher (1976) proposed an informal designation of the sequence as Rio das Velhas greenstone belt, whereas Ladeira (in Loczy and Ladeira, 1976) proposed the formal Rio das Velhas Supergroup designation to include the volcano–sedimentary sequence. Schorscher (1978) described komatiitic flows at the base of the sequence, naming them the Quebra Osso Group (Schorscher, 1979). Ladeira (1980) divided the Nova Lima Group into metavolcanic (lower), chemical metasedimentary (intermediary) and clastic metasedimentary units (upper). Based on the lithofacies associations described by Pedreira and Silva (1996) and Baltazar and Pedreira (1996, 1998), the most recent mapping of the Rio das Velhas greenstone belt (Baltazar and Silva, 1996; Zucchetti and Baltazar, 1998) subdivided the Nova Lima and Maquiné Groups into informal lithostratigraphic units (Fig. 2; Table 1).

Although primary sedimentary and igneous structures are preserved in many places, subdivision of the

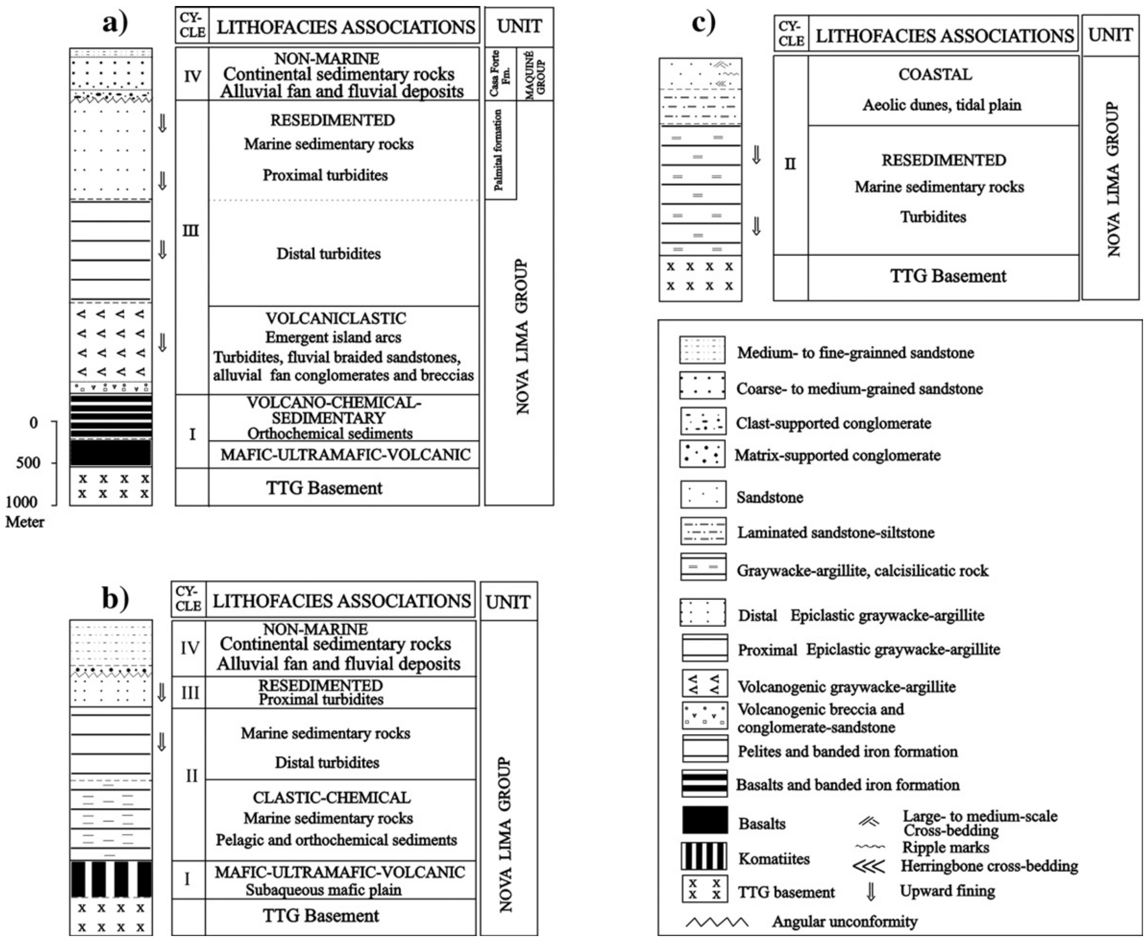

Fig. 3. Composite stratigraphic columns of the Nova Lima–Caeté (a), Santa Bárbara (b) and São Bartolomeu c) blocks.

sequence into lithostratigraphic units was not attempted, because the identification of facing and their actual thicknesses are modified by superimposed deformations. Only the existing formal lithostratigraphic subdivision was maintained (proposed by Dorr et al., 1957; Dorr, 1969).

In order to describe the stratigraphy, the approach of Eriksson et al. (1994) for Archean terrains is used. It subdivides the strata into genetic packages, independently from their lithologic groupings, each of them defining a distinct stratigraphic and tectonic system. This approach resulted in the recognition of the lithofacies associations discussed below, with their stratigraphic relations deduced from field relations and limited geochronology. This results in the recognition of four sedimentary cycles, with or without associated volcanism, defined by their dominant lithofacies. The spatial distribution of these cycles is controlled by shear zones, which juxtaposed tectonic blocks with distinct lithostructural characteristics, making it impossible to incorporate all of the sequences in a single stratigraphic column (Fig. 3). These are the Nova Lima–Caeté, Santa Bárbara and São Bartolomeu tectonic blocks (Fig. 4). The Nova Lima–Caeté block, in the northern sector of the area, is separated from the São Bartolomeu block, to the south, by the Bem-Te-Vi thrust fault and by the southern sector of the São Vicente–Raposos shear zones. The Santa Bárbara block, in the east, is separated from the Nova Lima–Caeté block, to the west, by the Fundão thrust fault.

There are few studies about the greenstone belt metamorphism, and they consider the rocks of the QF region to have undergone three metamorphic events (Dorr et al., 1957; Dorr, 1969; Ladeira, 1980). The first event, prior to the greenstone sequence formation, affected the TTG gneisses with migmatization at high grade metamorphism. A second event affected the Rio das Velhas Supergroup with greenschist and low amphibolite facies metamorphism at about 2700 Ma (Herz, 1970, 1978). The last event affected the Supergroup Minas with greenschist facies metamorphism at about 2000 Ma (Ladeira et al., 1983). Marshak and Alkmim (1989),

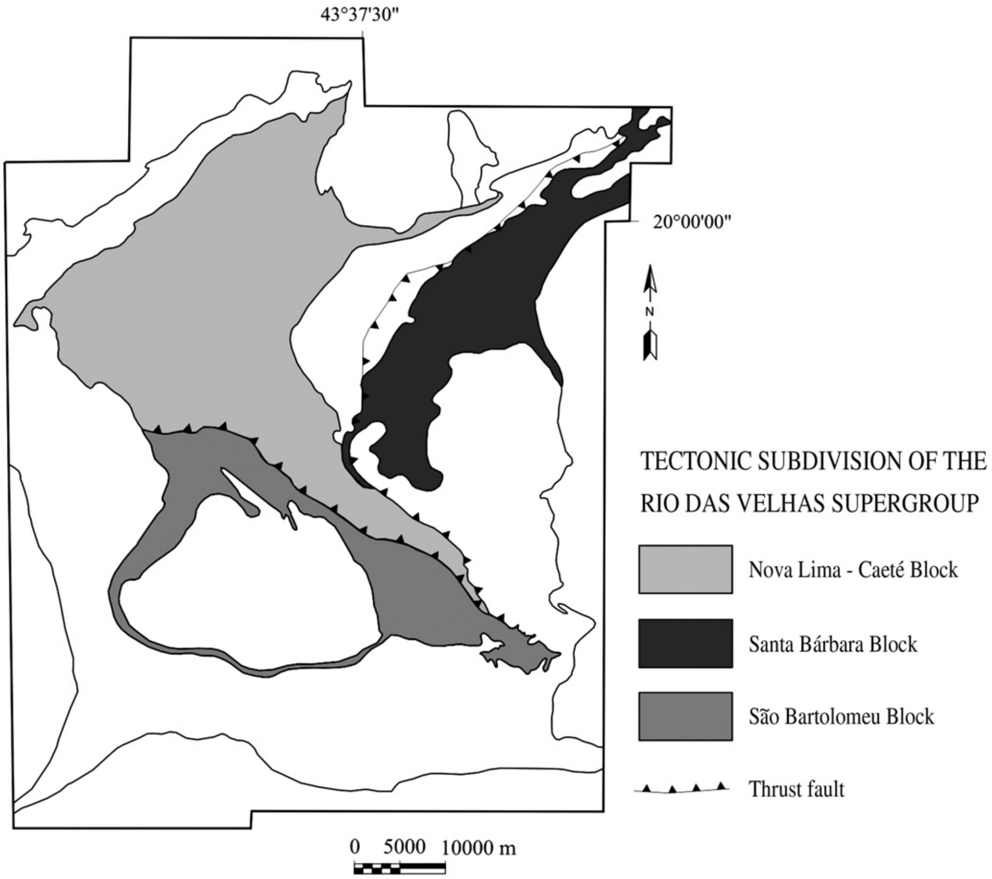

Fig. 4. Lithostructural domains of the Rio das Velhas greenstone belt (modified after Zucchetti and Baltazar, 1998).

however, stated that two regional prograde metamorphic events affected the Minas (and Rio das Velhas) Supergroup rocks in the QF region, the first associated with a Transamazonian compressional event at 2000 to 2200 Ma, and the second related to the Brasiliano Orogenic Event at 400 to 600 Ma.

The Rio das Velhas greenstone belt rocks are metamorphosed at greenschist facies in the Nova Lima–Caeté and Santa Bárbara blocks, and reached the amphibolite facies in the São Bartolomeu block. Metabasalts of the Nova Lima–Caeté and Santa Bárbara blocks show the assemblage actinolite + clinozoisite + chlorite + albite ± quartz ± carbonate ± biotite. Pyroxene is locally present, either in BIF, denoting an earlier, higher metamorphism, with greenschist facies retrograde metamorphism or only a single episode of greenschist facies metamorphism with higher grades conditions in places (Ladeira et al., 1983). The widespread preservation of delicate primary features, like fan texture and plagioclase with hollow cores in metabasalts (Zucchetti et al., 2000a), and the restricted occurrence of amphibolite facies parageneses, suggest metamorphism of greenschist facies with local amphibolite facies conditions for the northern sector of the QF. However, sedimentary rocks of the greenstone in the São Bartolomeu block are metamorphosed at the amphibolite facies, exhibiting the mineral assemblage quartz + chlorite + biotite ± staurolite ± kyanite ± sillimanite. Geothermometric studies in graywacke and pelite indicate regional metamorphism at middle greenschist facies to middle amphibolite facies, with greenschist facies retrograde metamorphism (Golia, 1997). The amphibolite facies minerals lie on the plane of the schistosity (D1), and are thus related to the first-generation structures described ahead in the paper, pre-dating the Minas Supergroup deposition. Therefore, an Archean metamorphic event is characterized, having reached the amphibolite facies in the São Bartolomeu block. Further metamorphic events provided the overall retrograde metamorphism of the sequence.

4. Lithofacies associations

The concept of sedimentary lithofacies associations has been widely used in Archean greenstone belts, mainly to determine the depositional environments of the sedimentary units and their source areas (Mueller et al., 1989; Eriksson et al., 1994; Jackson et al., 1994; Lowe, 1994). The application of the same concept to the volcanic rocks and knowledge regarding the deformation events make it possible to define the overall evolution of the volcano–sedimentary sequence. The lithofacies associations presented are essentially the same as those of Baltazar et al. (1994), Pedreira and Silva (1996), Baltazar and Pedreira (1996, 1998) and Zucchetti and Baltazar (2000), with only a few revisions and the additions.

4.1. Mafic–ultramafic volcanic lithofacies association

This association is predominantly composed of mafic and ultramafic lavas, with minor intrusions of gabbro, anorthosite and peridotite, and intercalations of banded iron formation (BIF), ferruginous chert, carbonaceous pelite, turbidites and rare felsic volcaniclastic rocks. The ultramafic lavas are represented by peridotitic komatiites, in massive or pillowed flows, in places brecciated and with spinifex texture (Schorscher, 1978; Sichel, 1983). Basalts dominate the association as massive and pillow flows (Fig. 5a), in places spilitized, with preserved primary textures such as varioles (Zucchetti et al., 2000a).

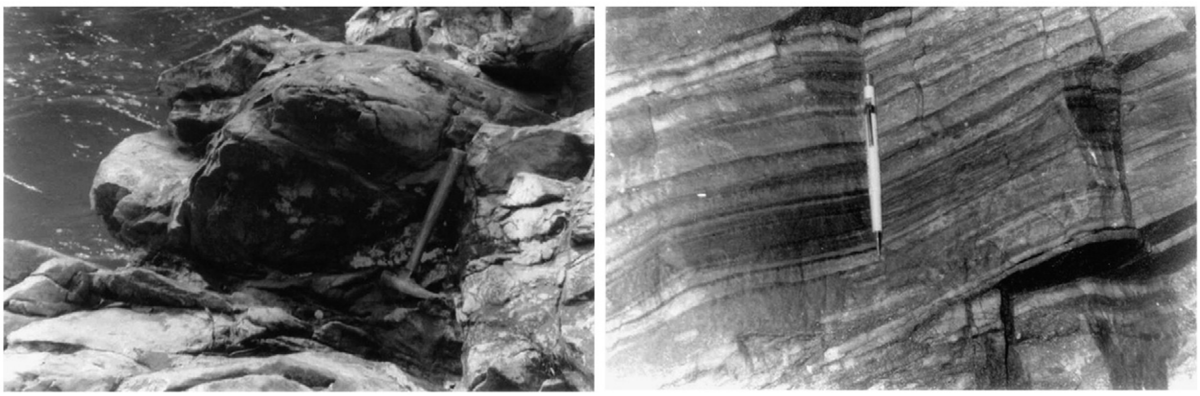

Fig. 5. (a) Pillowed tholeiitic basalt of the mafic–ultramafic volcanic association. (b) Banded iron formation of the São Bento gold mine, clastic–chemical–sedimentary association.

Following the geochemical classification of Sylvester et al. (1997), the basalts of this association are divided into tholeiites with <9 wt.% MgO, and high-Mg basalts with >9 wt.% MgO (Fig. 6). Rare earth elements (Fig. 7a) and binary plots of Mg, Ni, Zr, Y, Th and Ta for the high-Mg basalts show that they are the most primitive basalts. The high-Mg basalts have rare earth element (REE) patterns indicating that they formed from partial fusion of a mantle plume (Zucchetti, 1998; Zucchetti et al., 2000b); the subchondritic to chondritic La/Sm ratios (Fig. 6) endorse a mantle source (Sylvester et al., 1997). These basalts have the following geochemical similarities with those of submarine plateaus: (1) relatively low Th/Ta and La/Yb ratios (Condie, 1994); (2) small Ni decrease with falling Mg#, e.g., a Mg# of 65 corresponds to 164 ppm Ni (Condie, 1994); and (3) near-flat REE patterns (Fig. 7a) (Polat and Kerrich, 2000). The komatiites associated are further evidence for a plume origin of both volcanic rocks. Campbell et al. (1989) and Campbell and Griffiths (1992) suggested that the relationship between komatiites and basalts in Archean greenstones could be explained by a mantle plume source, in which the komatiites came from the hot plume tail and the basalts from the cooler head. Arndt et al. (1997) support this idea and conclude that Archean komatiites and basalts probably formed by melting in plumes, and the closest modern analogues are oceanic plateau basalts.

The MgO and trace element contents distinguish the tholeiites from the high-Mg basalts (Fig. 6). The tholeiites have more incompatible elements (e.g., Zr, Y, Th, Ta, Nb) and REE concentrations, with a LREE enrichment (Fig. 7b). On the basis of incompatible

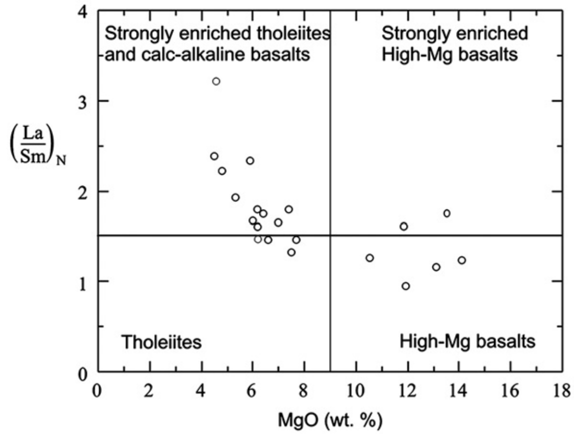

Fig. 6. Concentration of MgO (wt.%) versus chondrite normalized La/Sm ratio (Sylvester et al., 1997). Basalts of the mafic–ultramafic volcanic and volcano–chemical–sedimentary associations. Data from Zucchetti (1998). Chondrite values after Anders and Grevesse (1989).

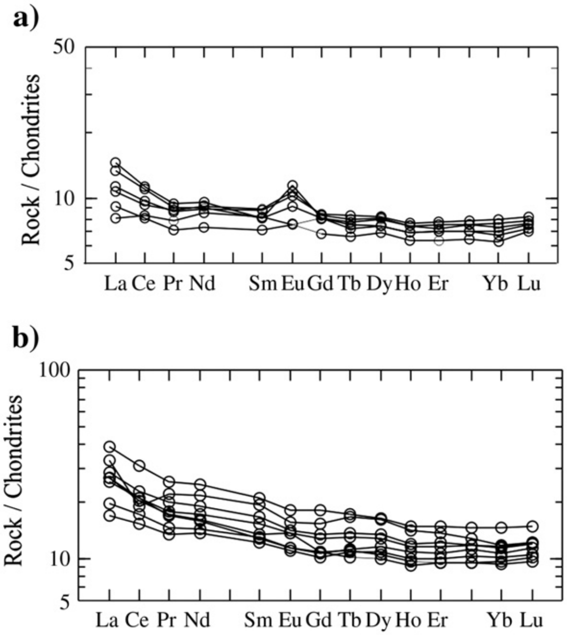

Fig. 7. Chondrite-normalized REE patterns of basalts from Rio das Velhas greenstone belt. (a) Mafic–ultramafic volcanic association: high-Mg basalts. (b) Mafic–ultramafic volcanic and volcano–chemical–sedimentary associations: tholeiitic basalts. Data from Zucchetti (1998). Chondrite values from Sun and McDonough (1989).

elements ratios, the tholeiites are divided into: (1) basalts with super-chondritic La/Sm ratios (Fig. 6) and high Th/Ta and La/Yb ratios, similar to arc-related basalts (Condie, 1994), and (2) basalts with Th/Ta and La/Yb ratios (~10) near the average for the upper Archean continental crust, suggesting contamination of basalts by continental crust, metasomatism by fluids rising from descending slabs or mixing of depleted with enriched mantle sources (Condie, 1994). The tholeiites have been interpreted as differentiated terms evolved by fractional crystallization from high-Mg basalts (Zucchetti, 1998; Zucchetti et al., 2000b). However, the tholeiites are here interpreted as related to island arcs, with no relationship to the high-Mg basalts.

4.2. Volcano–chemical–sedimentary lithofacies association

This association is made up of tholeiites (Figs. 6 and 7b) intercalated with abundant BIF and ferruginous chert, and less fine, clastic sedimentary rocks, such as carbonaceous turbidites and pelites; pelites are intercalated with chemical sedimentary rocks. The basalts are mainly massive flows, with amygdaloidal, sub-ophitic and micrographic textures, and locally gabbroic textures

(Zucchetti et al., 2000a). On the basis of incompatible elements ratios, the tholeiites have a geochemical affinity of arc-related basalts, showing basalts with super-chondritic La/Sm ratios (Fig. 6) and high Th/Ta and La/Yb ratios (Condie, 1994). Despite having < 9 wt.% MgO and LREE enrichment, some tholeiites present chondritic La/Sm ratios (Fig. 6) and low Th/Ta and La/Yb ratios similar to submarine plateau basalts derived from mantle plumes, like the high-Mg basalts of the mafic–ultramafic volcanic association. The abundance of chemical sedimentary rocks indicates more quiescent periods than for the mafic–ultramafic volcanic association. The mafic–ultramafic volcanic and volcano–chemical–sedimentary lithofacies associations are closely associated. They are transitional, a feature determined by an increase in chemical sediments associated with the mafic and ultramafic lavas of the former. The petrographic and chemical characteristics of the basaltic flows of both associations, and the nature of their sedimentation, are typical of deposition in a deep sea environment.

4.3. Clastic–chemical–sedimentary lithofacies association

This association is typified by alternating fine-grained, clastic and chemical sedimentary rocks. Pelites (micaceous and chloritic schists) are intercalated with lesser BIF and subordinate chert and carbonaceous schists. The pelites are layered on a millimeter to decimeter scale and are generally intercalated with dark gray, carbonaceous phyllite layers of variable thickness. The BIF in the São Bento Au deposit (Fig. 5b), for

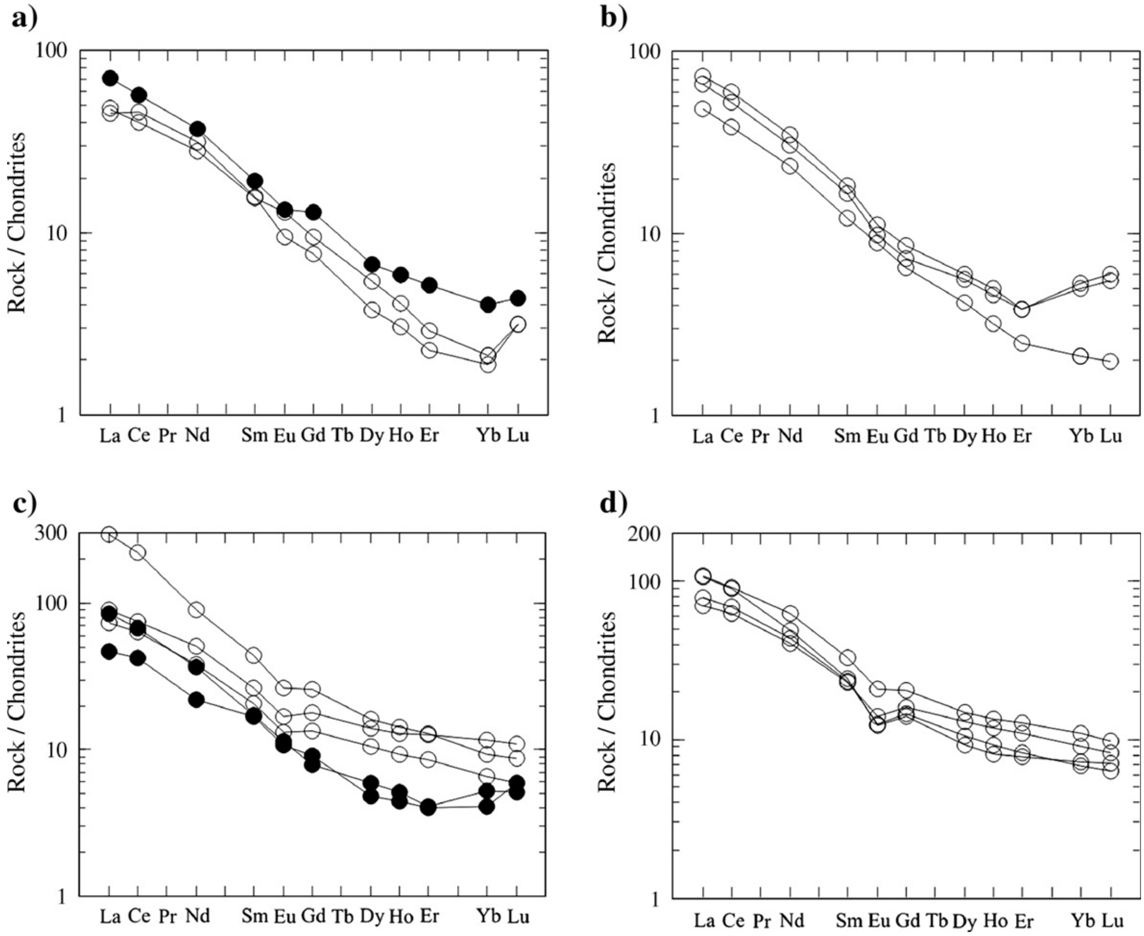

Fig. 8. Chondrite-normalized REE patterns of rocks from the Rio das Velhas greenstone belt. (a) Volcaniclastic association: monomictic breccias (○) and dacite (●). (b) Resedimented association, graywackes of northern sector at greenschist facies. (c) Resedimented association, graywackes of northeastern sector at greenschist facies. The severe depletion in HREE (●) indicates felsic source area, the slight depletion in HREE (○) may be derived by mixing of felsic and mafic source areas. (d) Resedimented association, graywackes of southern sector at amphibolite facies. Data from Silva (1996, 1998). Chondrite values from Sun and McDonough (1989).

example, is oxide facies, with variable proportions of quartz, magnetite and carbonates, and contains pelitic layers that exhibit chlorite and stilpnomelane (Martins Pereira et al., 2007-this volume). The clastic–chemical–sedimentary association could have been deposited during periods of interruption of basaltic flows or, laterally, in a deep-water pelagic environment, away from volcanic centers. The association was deposited in a submarine environment, following the basic–ultrabasic volcanism. This lithofacies association is transitional to distal turbidites included in the resedimented lithofacies association.

4.4. Volcaniclastic lithofacies association

This association is made up of volcaniclastic felsic and mafic rocks. Subordinate dacitic lenses are tectonically intercalated with basaltic flows, and have an adakitic

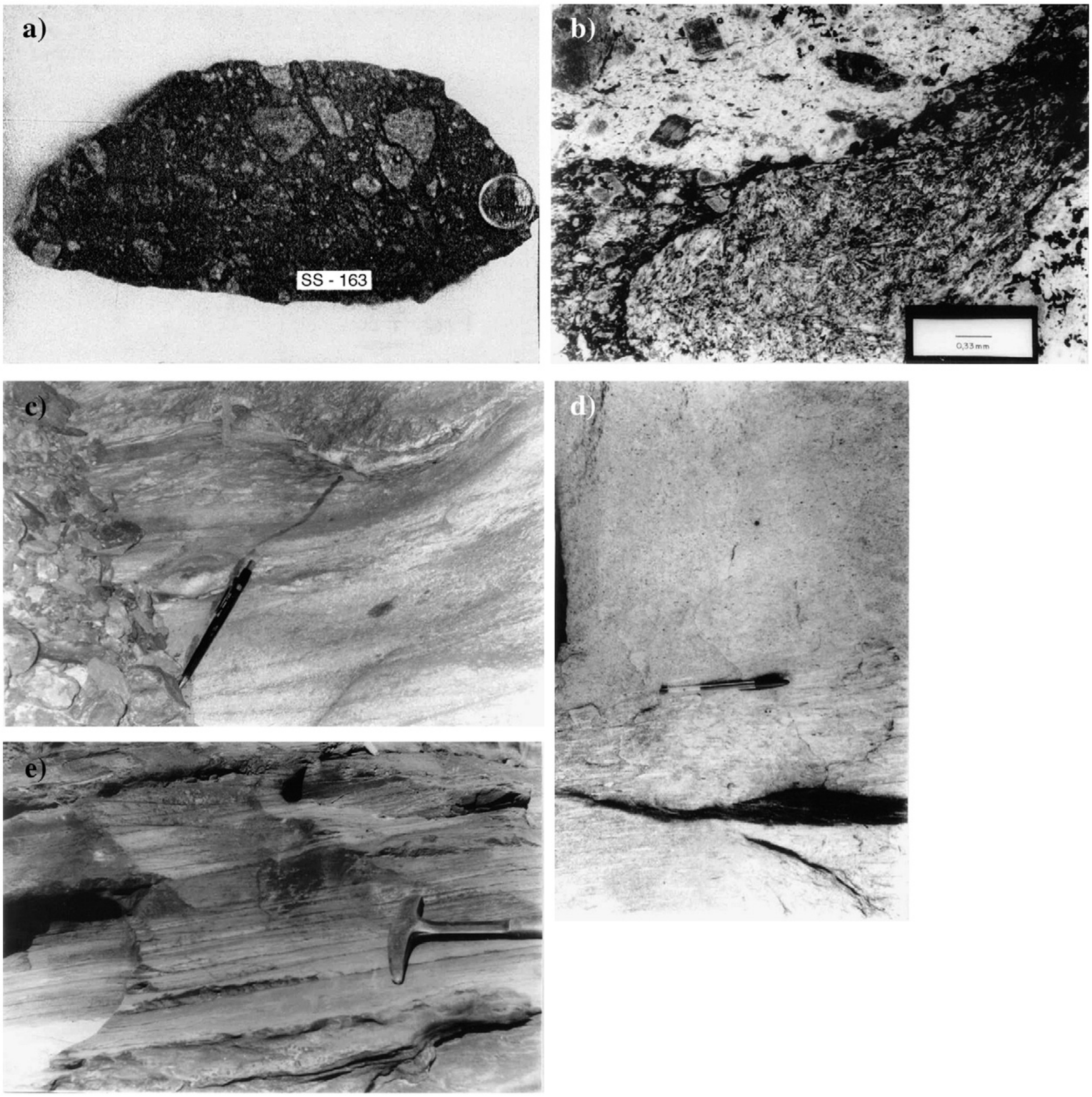

Fig. 9. Volcaniclastic association. (a) Monomictic breccia with dacitic fragments. (b) Polymictic breccia containing dacite (upper part) and basalt (lower part) clasts, plane-polarized light. (c) Conglomerate–graywacke lithofacies. (d) Graywacke–sandstone lithofacies. (e) Turbidite of the graywacke–argillite lithofacies.

composition, according to Silva et al. (2000). The dacites have a porphyritic texture, with euhedral plagioclase and less hornblende phenocrysts in a matrix of recrystallized quartz and plagioclase, and oriented sericite and chlorite (Zucchetti et al., 2000a). The dacites have a strongly fractionated REE pattern and strong HREE depletion (Fig. 8a), consistent with partial melting of basaltic rocks at mantle depths where garnet is a stable residual phase (Fig. 7.6a in Taylor and McLennan, 1985). The dacites REE pattern is similar to REE pattern of felsic volcanic rocks (FEL-2) of the Central Hearne supracrustal belt (Western Churchill Province, Canada), which matches the slope of melt derived from garnet-bearing amphibolite (Sandeman et al., 2004).

The volcaniclastic rocks comprise four lithofacies: (1) monomictic and polymictic breccias, (2) conglomerate–graywacke, (3) graywacke–sandstone, and (4) graywacke–argillite. Lithofacies (1) and (2) occur in the same area in the NE sector, whereas lithofacies (3) and (4) are intimately associated in two other areas in the W sector of the greenstone belt (Fig. 2). They were grouped together in the same association because they are similar in composition and texture, having a felsic volcanic contribution to the sediments source. The monomictic breccias have a sandy matrix containing dacite fragments (Fig. 9a), whereas the polymictic breccias have a clay-rich matrix, with fragments of basalt and dacite (Fig. 9b). Both are matrix supported with predominantly angular, poorly sorted fragments; the matrix of monomictic breccias is felsic, whereas the matrix of polymictic breccias is mafic. The conglomerate–graywacke lithofacies consists of interbedded graywackes, sandstones and grain-supported conglomerates with rounded and poorly sorted dacitic pebbles (Fig. 9c). Lithofacies (1) and (2) are characteristic of an upper to middle-alluvial fan environment. The graywacke–sandstone lithofacies (Fig. 9d) is intimately associated with the graywacke–argillite lithofacies. It is made up of cycles of upward fining graywacke–sandstone, about 1 m thick, with basal graywackes containing lithic fragments and quartz and plagioclase crystals, grading into medium- to fine-grained sandstones at the top of the cycles. Trough and planar cross-bedding are common features of sandstones, with sigmoidal cross-bedding occurring locally. These textural and structural features are typical of a fluvial environment. The matrix, fragments and grains, mainly of the graywacke fraction, are clearly of volcanic origin, providing a link with the adjacent graywacke–argillite lithofacies which was deposited by turbidity currents. The graywacke–argillite lithofacies is varied in composition and upward fining (Fig. 9e). The variation is progressive and cyclical, and the layers have millimeter to centimeter thicknesses. This lithofacies was deposited by turbidity currents in a submarine environment. Rare earth elements analysis of monomictic breccias reveals patterns similar to dacitic lavas (Fig. 8a), and corresponding to McLennan and Taylor's (1991) Type 2 turbidites; their $Gd_N/Yb_N > 2.0$ and they derived from a felsic source, such as Na-rich volcanic or granitic rocks. The occurrence of dacitic pebbles and volcanic crystals, the lack of plutonic fragments and the REE patterns suggest that felsic volcanic rocks were the main source for the sedimentary rocks. Graywacke–argillite lithofacies of this association grades into epiclastic graywackes of the resedimented association.

4.5. Resedimented lithofacies association

This association is widely distributed in the QF, and includes three different sequences of graywacke–argillite, two metamorphosed in the greenschist facies in the N and E sectors, and one in the amphibolite facies in the southern.

The lithofacies in the N and E sectors are composed mainly of graywackes, quartz graywackes, sandstones and siltstones, with cyclic layers and abrupt basal contacts between cycles (Fig. 10). These are up to 0.5 m thick, and exhibit upward fining, with coarse sand containing granules at the base and grading to carbonaceous clay at the top. Some cycles are composed of fine sand and clay, with pelagic facies of BIF. Other lithofacies are of fine sandstones or siltstones with cross-bedding, alternating with sand and clay, in centimeter-scale cycles cut by channels. Planar cross-bedding, plane and trough bedding are common structures in silty and sandy layers. Incomplete Bouma (1962) divisions, with cycles of the common types Tb-d-e, Tc-e, Ta-b-d, Tb-c-

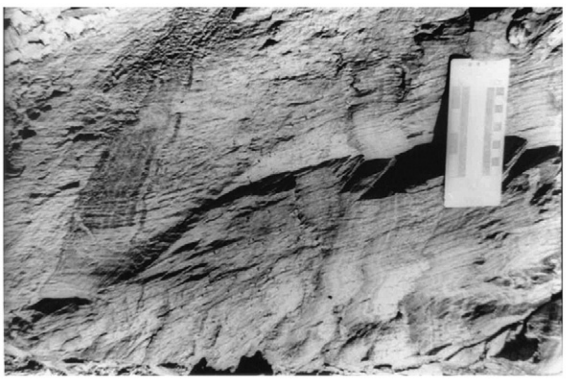

Fig. 10. Graywacke–carbonaceous pelite turbidite showing rhythmic bedding, with upward-fining graded bedding cycles.

d-e and Td-e, occur together. The features of this association indicate that it was deposited by turbidity currents (Selley, 1988) of high and low densities (Mutti, 1992), representing proximal sand (TS) and distal mud (TM) turbidites according to the nomenclature of Einsele (1992). Although they are texturally, structurally and compositionally similar, these graywackes have distinctive REE patterns. Those of the northern sector derive from a felsic source, with strongly fractionated REE and depletion in HREE (Fig. 8b), similar to the Type 2 turbidites of McLennan and Taylor (1991); they have $Gd_N/Yb_N > 2.0$ and derive from a Na-rich felsic source. Graywackes in the E sector, in turn, display two different REE patterns (Fig. 8c). They can be enriched in LREE, with a moderate depletion of HREE and slight negative Eu anomaly, corresponding to the McLennan and Taylor's (1991) Type 1 turbidites; these are interpreted as deriving from a mafic and K-rich felsic volcanic source (mixed source). The other eastern turbidites have REE patterns suggesting that the sources were Na-rich felsic volcanic and/or granitic rocks, similar to Type 2 turbidites of McLennan and Taylor (1991). The northern graywackes are transitional to volcaniclastic turbidites of the volcaniclastic association. The eastern graywackes grade into fine-grained sediments of the clastic–chemical–sedimentary association.

The graywacke–argillite sequences of the southern sector, at amphibolite facies, commonly have intercalations of calc–silicate rocks and BIF. They are plane- to cross-bedded graywacke–argillite successions with upward-fining cycles, centimeter to decimeter in thickness, with abrupt bases. There are local intercalations of polymictic conglomerate lenses in a graywacke matrix (Golia, 1997) that have normal to inverse grading, with pebbles of dacite, trondhjemite and quartz grains (Zucchetti et al., 1996, 1998). Some petrographic characteristics of the graywacke–argillite sequences, such as bipiramidal quartz and corroded crystals, indicate a major volcanogenic contribution. According to Pedreira and Silva (1996) and Baltazar and Pedreira (1996, 1998), conglomerates can be correlated with Mutti's (1992) very coarse-grained facies type, and resulted from the erosion of conglomerates deposited previously by hyperconcentrated flows. These graywackes show REE patterns similar to McLennan and Taylor's (1991) Types 1 and 2. The former displays LREE enrichment, slight HREE depletion and negative Eu anomaly (Fig. 8d), indicating a mixed origin of mafic and K-rich felsic sources. The Type 2 turbidites, with a Na-rich felsic source area (Golia, 1997), have conglomerate intercalations with pebbles of dacite and trondhjemite, indicating contributions from both volcanic and plutonic rocks. These graywackes are transitional to sandstone–siltstone lithofacies of the coastal association.

4.6. Coastal lithofacies association

This association is restricted to a small area northwestern of the Bação complex, and combines four lithofacies: (1) sandstone with medium- to large-scale cross-bedding; (2) sandstone with ripple marks; (3) sandstone with herringbone cross-bedding, and (4) sandstone–siltstone.

The sandstones of lithofacies (1) have planar and trough cross-beddings related to Allen's (1963) Xi type, with cuneiform terminations (Fig. 11a), interpreted as dune of the barchan type by Pedreira and Silva (1996). An eolian environment (Pedreira and Silva, 1996) is suggested by bimodal grain size, apparently without internal cross-lamination, exhibiting ondulation of small amplitude and large wavelength, and ripple index higher than 10 (Tucker, 1996). Lithofacies (2) has asymmetric straight-crested ripple marks (Allen, 1968), with the ratio wavelength versus amplitude providing a ripple index of about 5 (Fig. 11b). These characteristics suggest deposition in shallow water and the proximity to lithofacies (3), and that they were subjected to the influence of tidal currents. Lithofacies (3) shows bidirectional flow (Fig. 11c) with variations of the tidal cycles in a subacqueous environment (Pedreira and Silva, 1996; Baltazar and Pedreira, 1996, 1998). It displays local sigmoidal and tidal bundle cross-bedding. The sandstone–siltstone lithofacies (4) were probably deposited in a shallow marine environment, tide plain facies (Féboli and Signorelli, 1996); it has planar and trough cross-beddings, where quartz and feldspar clasts preserve volcanogenic features.

4.7. Non-marine lithofacies association

This association corresponds to the Casa Forte Formation of the Maquiné Group, and occurs in the central and eastern sectors of the QF. It is made up of the lithofacies: (1) conglomerate–sandstone; (2) coarse-grained sandstone, and (3) fine- to medium-grained sandstone.

The conglomerate–sandstone lithofacies is dominated by clast-supported polymictic conglomerates (Fig. 12a) intercalated with sandstones. The pebbles are rounded or planar/flattened, in places imbricated, comprising quartz vein, sandstone, ferruginous sandstone, BIF, siltstone and pelite, of up to 30-cm diameter. The sandstones are medium-grained, massive, plane-bedded or with trough and planar cross-bedding. Upward-fining graded cycles

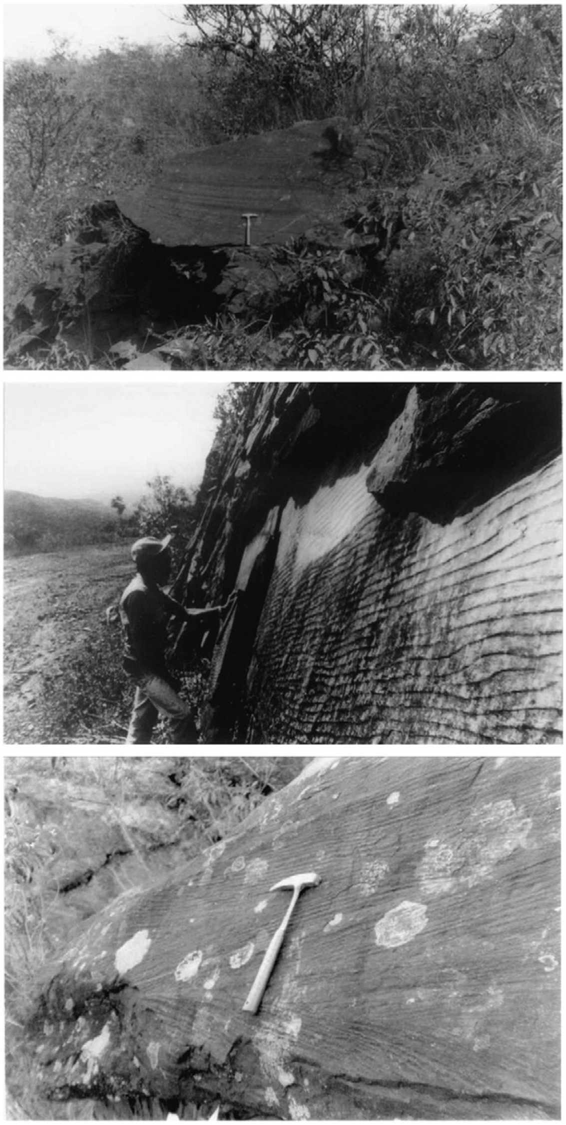

Fig. 11. Coastal association. (a) Cuneiform trough cross-bedding in sandstone. (b) Sandstone with asymmetric ripple marks. (c) Sandstone with herringbone cross-bedding.

of 0.50-m thickness and scour-and-fill channel structures are other common features of these sandstones. The association of clast-supported conglomerates with cross-bedded sandstones is characteristic of alluvial–fluvial fan deposits. The clast-supported conglomerates are, therefore, interpreted as longitudinal bars, the sandstones with plane bedding as top bar deposits, the sandstones with trough cross-bedding as channel-fill deposits, and sandstones with planar cross-lamination as linguoid bars (Pedreira and Silva, 1996). This lithofacies may, therefore, be correlated to the mid-fan area of alluvial fans of a braided fluvial system. In the eastern of the area, matrix-supported polymictic conglomerates (Fig. 12b) are interbedded with sandstones. Pebbles and boulders, up to 30 cm in diameter, are of quartz vein, BIF, chert, and mafic and felsic volcanic rocks. These rocks are interpreted as more proximal deposits within the alluvial fans, deposited during the waning stages of current flow.

Lithofacies (2) is made up of coarse-grained sericitic sandstones (Fig. 12c), laminated or with planar bedding. It

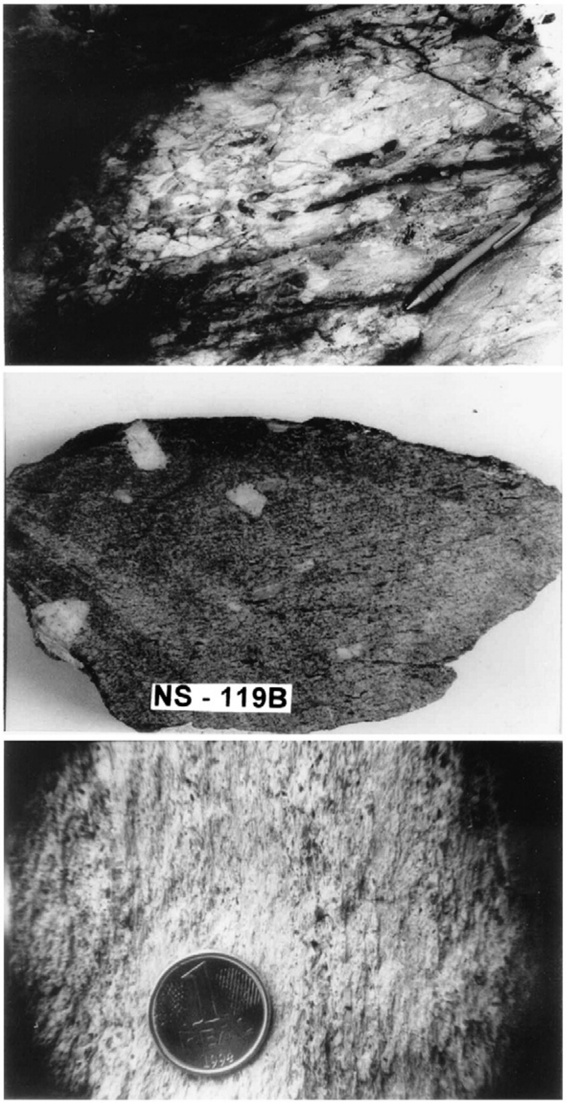

Fig. 12. Non-marine association. (a) Polymictic conglomerate with clasts of banded iron formation, carbonaceous schist, quartz vein and sandstone. (b) Matrix-supported conglomerate. (c) Coarse-grained sericitic sandstone.

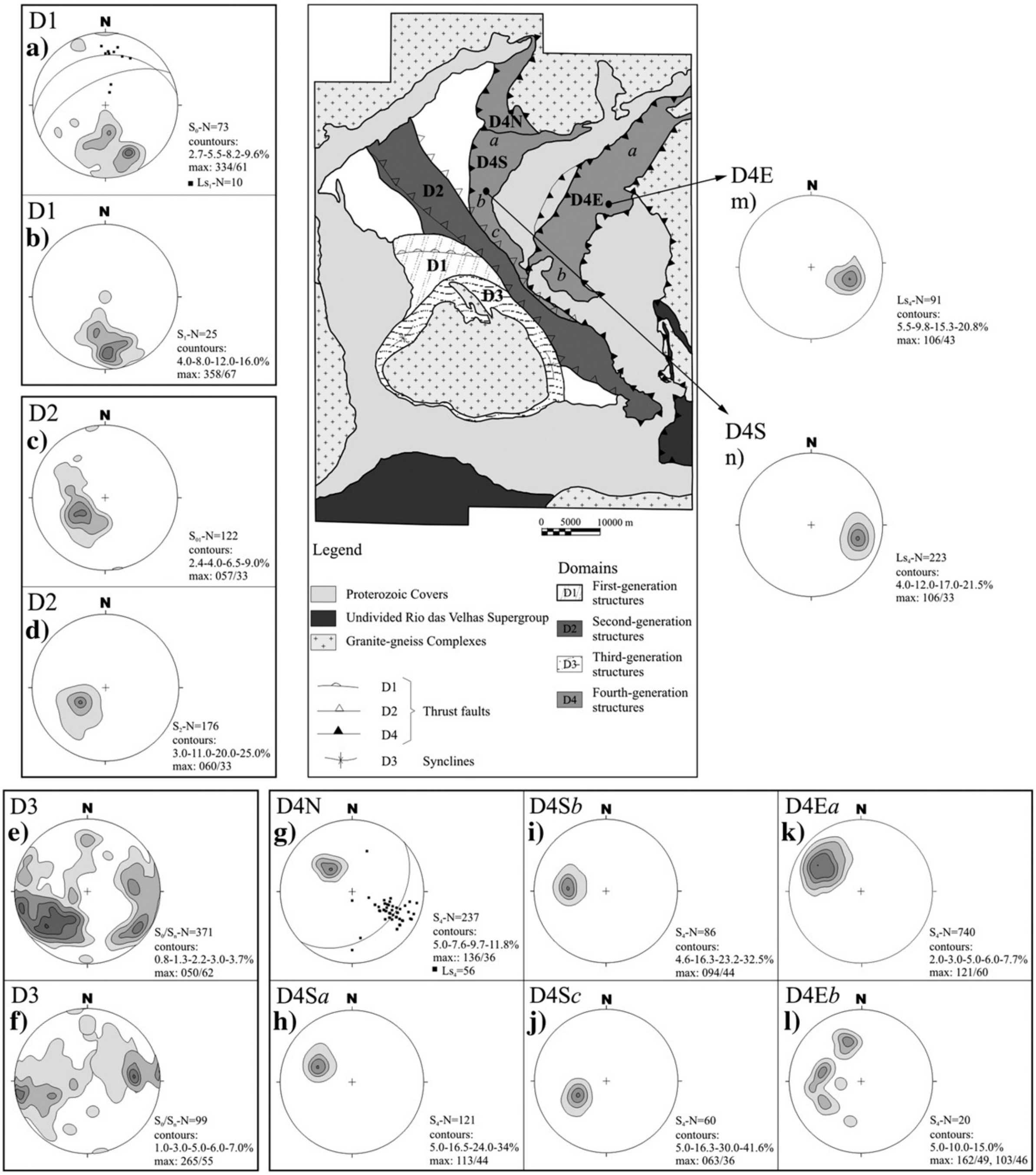

Fig. 13. Structural domains of the Rio das Velhas greenstone belt and respective stereograms: (a–b) Domain D1, poles to S_0 with Ls_1 and poles to S_1; (c–d) Domain D2, poles to S_0 and poles to S_1; (e–f) Domain D3, poles to S_n around the Bação complex and pole to S_n in the eastern marginal syncline; (g) Domain D4N, poles to S_4 with Ls_4 (stretching lineation) of the northern segment of the Ribeirão da Prata–Caeté fault system; (h, i, j) Domain D4S, poles to S_4 of the obliques and frontal ramps of the Ribeirão da Prata–Caeté fault system; (k–l) Domain D4E, poles to S_4 of the oblique and frontal ramps of the Fundão–Água Quente fault zones; (m–n) Domains D4E and D4S, stretching lineations.

is described by Baltazar and Pedreira (1996, 1998) as a micro-conglomeratic sandstone lithofacies. According to these authors, the main feature is the graded bedding in upward-fining cycles, commonly with lenses and layers of polymictic conglomerates similar to the previous lithofacies at its base. The cycles are 0.2- to 1.50-m-thick, with eroded bases, varying from sand to silt–clay at the top. Small- to medium-scale trough and planar cross-beddings are common; scour-and-fill channel structures also occur. This lithofacies was interpreted (Baltazar et al., 1994; Baltazar and Pedreira, 1996, 1998) as distal, not confined flow deposits of a braided plain river system.

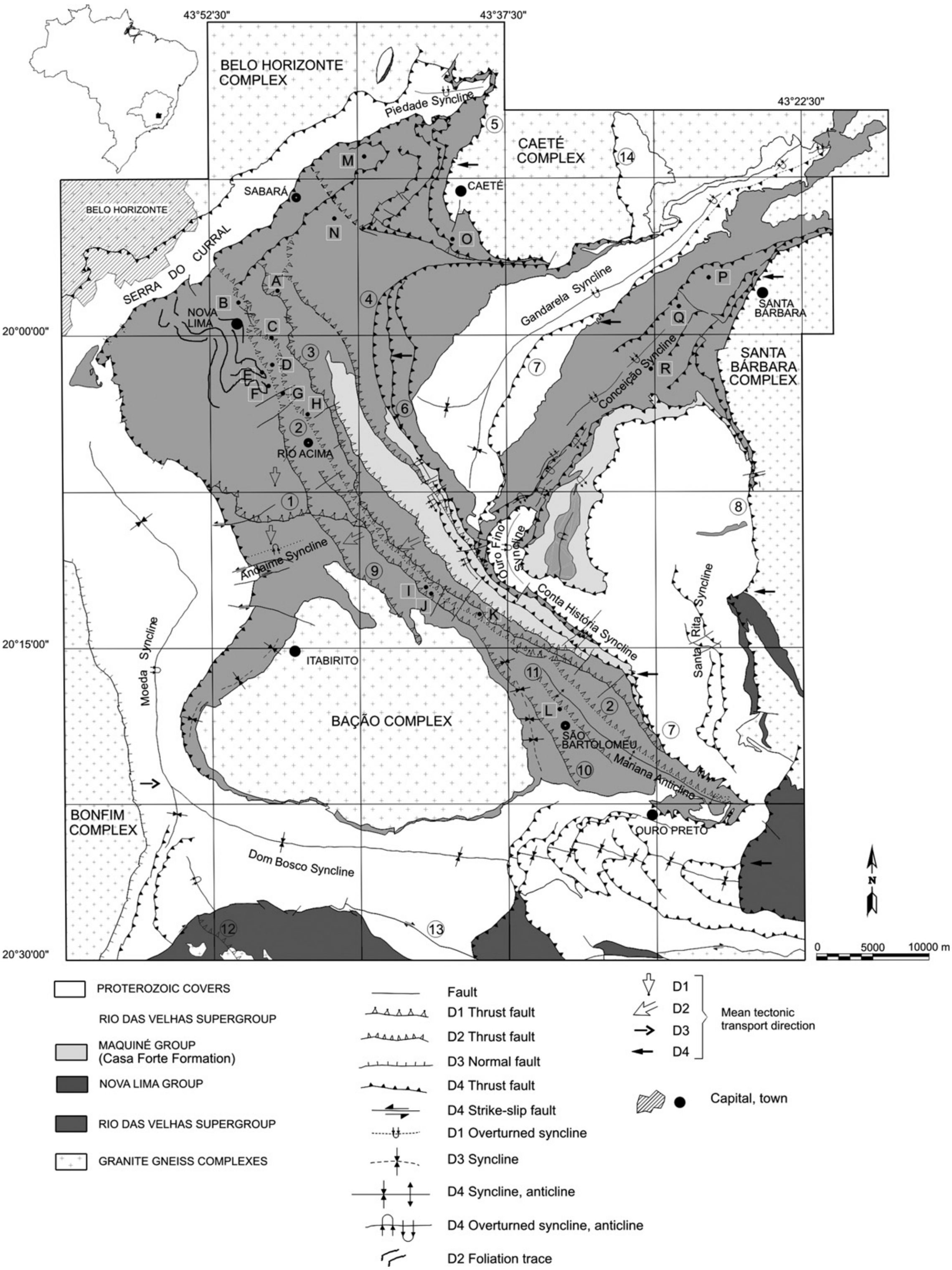

Lithofacies (3) is made up of impure sandstones with planar cross-beddings and small-scale troughs. Upward-fining graded bedding, in 0.1- to 0.5-m-thick cycles, are also interpreted as distal deposits of a braided plain.

5. Structural geology

The structural history of the Rio das Velhas greenstone belt is discussed below. The area has been divided in four structural domains, defined by their structural styles and according to the trend of their main megascopic structures (Fig. 13). In each domain, a certain group of planar and linear structures are well preserved, and related to at least four generations of structures that resulted from three deformational events affecting the greenstone belt. The first and second generations are attributed to an Archean and contractional event, the third generation is extensional and attributed to a Paleoproterozoic event, and the fourth is contractional and of Neoproterozoic age (Baltazar and Zucchetti, 2000).

5.1. First-generation structures (D1)

The first-generation structures are well preserved in the southern sector of the QF, in structural domain 1 (Fig. 13). The main regional D1 structures include E-striking and N-dipping thrust faults (Fig. 14), and open subhorizontal flexural normal folds to S-verging and ENE-plunging tight to isoclinal folds. Mesoscopic structures include (1) a NE-striking bedding (Fig.13a), (2) S_0 folds with an associated S_1 axial planar foliation, mylonitic in high strain zones (Fig. 13a,b), and (3) mineral and stretching lineations (Ls_1) on S_0 and S_1 (Fig. 13a). The Bem-Te-Vi thrust is the most prominent regional structure. It is a low-angle, N-dippping narrow mylonitic foliation zone, with a downdip stretching lineation that juxtaposes terrains of contrasting geological characteristics (Fig. 2). The Serra dos Andaimes, constituted by sandstones of the coastal lithofacies association, is here interpreted as the core of a major S-verging overturned syncline, with axis plunging 055°/22° (Fig. 13a). The Andaimes syncline (Fig. 14) is defined by folding of bedding surfaces, with an associated axial planar foliation (S_1).

The structural geometry suggests a fold-thrust style deformation under a ductile non-coaxial regimen. The D1 structures represent a single major subhorizontal, compressional, north–south shortening episode, with a north-side-up component of displacement. This episode is Late Archean affecting only the Nova Lima Group. It is younger than 2749 Ma, U–Pb date from detrital zircon grains (Suita et al., 2002) of Serra dos Andaimes' sandstones and older than 2672 Ma, age of gold mineralization (Lobato et al., 2007-this volume), which is related to overprinted D2 deformation. Structural features related to this deformation are described by Rynearson et al. (1954), Dorr (1969), Ladeira and Viveiros (1984), Corrêa Neto et al. (1994), Baltazar (1996, 1998) and Baltazar and Zucchetti (2000).

5.2. Second-generation structures (D2)

These structures are preserved in the central portion of the QF, corresponding to domain 2 (Fig. 13). Major D2 structures are NW-striking thrust faults, and associated overturned tight to isoclinal NW trending folds, verging to SW. The foliation S_2 is axial planar of folds defined by S_0/S_1 and evolves to a transposed foliation and to mylonite in the more deformed zone, with an average orientation 060°/35° (Fig. 13c, d).

The main thrusts are the Acuruí, Córrego Areão, Tapera, São Vicente and Raposos fault (Fig. 14). They are ductile shear zones, generated in a non-coaxial regimen, marked by zones of mylonites and a stretching lineation. Plunges of the stretching and mineral lineations range between 070/25 (Féboli and Signorelli, 1996) and 060°/20° (Oliveira et al., 1997). Thrusts have an important sinistral strike–slip component overprinted by a reactivation during the Neoproterozoic west-vergent compressional event (fourth-generation structures: D4). In Serra dos Andaimes, center-west of the QF, D2 thrusts truncate and dislocate D1 structures (Fig. 14). Clasts of deformed rocks in basal conglomerates of the Casa Forte Formation (Maquine Group) support a previous D1 deformation phase of the underlying Nova Lima Group (Atlas V. Corrêa Neto, personal communication, 2000). Also, northeast of the Rio Acima town the Casa Forte Formation is in an angular unconformity over the Palmital Formation, top of the Nova Lima Group. D2 structures are also preserved west of Caeté town (Fig. 14).

Fig. 14. Structural map of the Quadrilátero Ferrífero showing the main structures of the Rio das Velhas greenstone belt (modified after Baltazar and Zucchetti, 2000). Faults: (1) Bem-Te-Vi, (2) São Vicente, (3) Raposos, (4) Ribeirão da Prata, (5) Caeté, (6) Cambotas, (7) Fundão, (8) Água Quente, (9) Acuruí, (10) Córrego Areão, (11) Tapera, (12) Congonhas, (13) Engenho, (14) Córrego do Garimpo. Gold deposits: (A) Raposos, (B) Morro Velho, (C) Bela Fama, (D) Bicalho, (E) Faria, (F) Morro da Glória, (G) Urubu, (H) Engenho D'Água, (I) São Vicente, (J) Paciência, (K) Cedro, (L) Tapera, (M) Cuiabá, (N) Lamego, (O) Juca Vieira, (P) Santa Quitéria, (Q) São Bento, (R) Córrego do Sítio.

There is a general spatial relationship between gold deposits and shear zones of this deformation. Au-bearing hydrothermal alteration zones are closely related to these shear zones. The São Vicente thrust is marked by the Morro Velho, Bela Fama, Bicalho, Urubu, Engenho D'Água, São Vicente, Paciência and Cedro gold deposits (Baltazar, 1996, 1998). The Raposos gold deposit is associated with the Raposos thrust fault, whereas Faria and Morro da Glória are also associated with shear zones of the same generation (Fig. 14). In some places, gold deposits are controlled by tear faults, ductile–brittle strike–slip shear zones, trending NE–SW, that transversely dislocate the D2 thrust fronts. The orebodies are parallel to the S2 milonitic foliation in the central portion of shear zones. A wide variety of structures may be mineralized including thrust faults, intersections of faults, sheath folds and hinge fold zones, subparallel to the L_2 stretching lineation in the more ductile environment, the general plunge of which is at about 040 to 060°/20 to 35°. However, the orebodies have a general east–west trending, orthogonal to the tectonic transport direction.

The D2 structures represent a compressional event, with southwest-verging structures. The S-C foliation patterns and displacement in shear zones indicate movement towards SW. The structural geometry and kinematic criteria suggest a fold-thrust style deformation under a ductile non-coaxial regimen. This deformation has affected both Nova Lima and Maquiné Groups. As these structures are covered by Proterozoic sedimentary rocks they are older than 2580 Ma (onset of Minas Supergroup deposition; Renger et al., 1994). The age is Late Archean and can be positioned at about 2672 Ma, age for gold mineralization (Lobato et al., 2007-this volume), which is related to this deformation. Structures related to this deformation are described by Noce et al. (1994), Corrêa Neto et al. (1994), Baltazar et al. (1995), Corrêa Neto and Baltazar (1995), Féboli and Signorelli (1996), Oliveira et al. (1997), Baltazar and Zucchetti (2000) and Lobato et al. (2001b).

5.3. Third-generation structures (D3)

Structures of this generation are related to a regional extensional event. Two main groups of structures are related to this extension. The first group of structures defines the quadrangle shape of the QF and is represented by the continuous regional synclines of the Serra do Curral, Moeda, Dom Bosco, and Santa Rita (and probably the Gandarela syncline). These synclines are defined by Proterozoic Minas Supergroup sedimentary rocks, deposited in an intracratonic environment during the extension (Chemale et al., 1994). The second group of structures is related to the domelike shape of the granite–gneissic basement that comprises the Belo Horizonte, Bonfim, Bação, Caeté, Santa Rita, and Santa Bárbara complexes (Fig. 2). The structures are associated with the uplift of the underlying granite–gneissic basement and consequent nucleation of the synclines.

The second group structural elements are well developed around the Bação complex, in the D3 structural domain (Fig. 13). The vertical uplift of the granite–gneissic body generated a S3 mylonitic border foliation and an associated surrounding down-dip mineral lineation, dipping outward from its center (Fig. 13e). Such uplift produced normal-sense movement shear zones around the complex and a reorientation of earlier fabrics in the adjacent greenstone cover (Fig. 13e). So, in the northern border of the Bação complex, the foliations plunge to the north, with kinematic indicators (S-C foliations, shear bands) both indicating reverse and normal movements, the latter overprinting the former. In the southern border, there are only indications of normal or transcurrent movements in the sedimentary rocks adjacent to the granite–gneissic complex. These vertical movements also generated marginal NE–SW to N–S trending subhorizontal upright synforms on the greenstone covers, respectively on the west and east sides of the Bação complex (Fig. 13f). Pre-existing mineral lineations and intrafolial folds were rotated to a subhorizontal plunge and a subvertical axis, respectively. These synforms were amplified by the superposed D4 W-vergent compressional event and converted in upright tight to isoclinal folds (Figs. 13 and 14; Corrêa Neto and Baltazar, 1995; Baltazar, 1996, 1998).

The geometric and kinematic arrangement of these structures is interpreted as due to the rise of domes against a pre-existing E-W-striking foliation, with a southward tectonic transport. A regional extension, in a ductile to ductile–brittle regimen, was responsible for the rise of the granite–gneissic basement blocks as metamorphic core complexes (Chemale et al., 1991, 1994; Baltazar et al., 1995; Baltazar and Zucchetti, 2000). Extensional faults such as that of the contact of the Moeda synclinal and the Bonfim complex (Fig. 14) (Endo and Nalini, 1992) are related to this event by Chemale et al. (1991, 1994). However, a Transamazonian NW-verging thin-skinned thrusting event, previous to this extensional phase, is proposed by Alkmim and Marshak (1998) and Marshak and Alkmim (1989). Folds and thrusts with the same attitudes of the contractional event of this model overprint D2 structures in the Cuiabá and Farias gold deposits regions (Fig. 14), and reorient partly the orebodies in this last deposit. These structures, here attributed to D4 W-verging deformation, can be correlated to this contractional event, but pieces of evidence are not clear inside the Quadrilátero Ferrífero. The subsequent orogenic collapse (2095 Ma, Sm–Nd whole-rock; Marshak et al., 1997) resulted in the development of a dome-and-keel structure (Marshak et al., 1992, 1993, 1997), instead of metamorphic core complexes, as accepted here.

5.4. Fourth-generation structures (D4)

The major D4 structure in the QF dominates the entire eastern sector, with a general N–S direction (Dorr, 1969; Ladeira and Viveiros, 1984; Marshak and Alkmim, 1989; Chemale et al., 1991, 1994; Corrêa Neto et al., 1994; Baltazar et al., 1995; Corrêa Neto and Baltazar, 1995; Baltazar, 1996; Endo, 1997; Baltazar, 1998; Alkmim and Marshak, 1998). It is the structural D4 domain in Fig. 13 and is regionally represented by well-developed N–S shear zones with mylonitic fabric, stretching lineation plunging towards ESE (Ls_4: Fig. 13m, n) and SxC kinematic markers indicate a west-verging thrusting. Thrusts are progressively younger from W to E, in a direction opposite to the tectonic transport (Baltazar et al., 1995) in a propagation of the overstep type (Butler, 1982). West-vergent tight to isoclinal folds with axial plane foliation (S_4) and dip-slip lineation are associated to the high strain zones. Outside these zones, folds become progressively open to gentle and parallel. The S4 foliation, with an east–southeast dipping, curves in map view to define a westwards convex arch, parallel with the related thrust system. Northern and southern ends represent oblique ramps (Fig. 13g, h, j, k, l) and have dextral and sinistral transpressive character, respectively. The central segments represent frontal ramps (Fig. 13i, l).

The Fundão–Cambotas shear system (Chemale et al., 1991; Endo and Fonseca, 1992), formed by the junction of the Fundão (Dorr, 1969) and Cambotas (Rodrigues et al., 1989) faults, is the main discontinuity. Other important thrusts are: the Ouro Fino, Flechas, Alegria, Frazão and Água Quente faults (Endo and Fonseca, 1992) to the east; and the Ribeirão da Prata and Caeté faults (Corrêa Neto and Baltazar, 1995), to the west. In the center-north of the area, an E–W trending fan-shaped mylonitic band, is an interference zone between the northern Caeté thrust front and the Ribeirão da Prata, to the south. The resulting E–W lateral ramp and moderate to gentle plunges south, with mineral and stretching subhorizontal lineations (Corrêa Neto et al., 1994; Corrêa Neto and Baltazar, 1995).

Northwest of Serra do Caraça, the Conceição syncline (Malouf and Corrêa Neto, 1996) is defined by bedding surfaces of the greenstone. This fold occupies the nucleus of the Conceição anticline (Dorr, 1969), defined by Minas Supergroup bedding surfaces, both northwest verging, with a subparallel axial trace. The internal syncline is interpreted as an old D1/D2 fold, with an ENE–WSW trending axis overlain unconformably by Minas Supergroup sedimentary rocks, amplified, rotated and inverted as a result of the compressive efforts from E to W of the D4 deformation, which generated the overlapping anticline. Subvertical, NS–EW trending crenulations and fracture cleavages are common, as late manifestations. Brittle faults which segment the thrust fronts are the latest manifestations of this event.

The structure geometry suggests a fold-thrust style deformation under a ductile–brittle non-coaxial regimen. The D4 structures represent a compressional event, with western-verging structures. Shear related S-C foliation patterns and displacements in the shear zones indicate movements towards west. The age is Neoproterozoic, an episode related to the Braziliano Orogenic Cycle (Chemale et al., 1991; Alkmim et al., 1994; Schrank and Machado, 1996a).

6. Gold deposits

Gold orebodies in the Rio das Velhas greenstone belt are structurally controlled and occur associated with hydrothermal alterations along D2 thrust shear zones, in a regional scale. The mineralizations are epigenetic and related to sulfide enrichment of host rocks, mainly BIF and the '*lapa seca*'. The latter is a quartz–carbonate-rich rock of controversial origin. The first accounts for 49%, and the second for 47%, of the contained gold; mafic–ultramafic, volcaniclastic and sedimentary rocks host the remaining 4% (Lobato et al., 2001b,c). The concentration of gold systems along D2 thrust shear zones suggests that mineralization is previous to onset of the Minas Supergroup sedimentary rocks deposition. Therefore, it is Archean in age.

Gold orebodies are hosted in small-scale structures within the larger deformation zones. In deposit-scale, gold deposits are controlled by second- and third-order NW–SE trending thrust shear zones, and ductile–brittle NE–SW trending strike–slip shear zones, that dislocate transversely the D2 thrust fronts. Cuiabá and Lamego deposits are controlled by large antiformal sheath folds (Vial, 1988; Vieira, 1992; Ribeiro-Rodrigues, 1998; Sales, 1998; Lobato et al., 2001a,c). At the orebody scale a great range of shear structures hosts alteration minerals zones which contain the gold associated: (a) brittle–ductile shear zone surfaces; (b) axial plane cleavage; (c) hinge fold zones; (d) sheath folds; (e) fracture cleavage; (f) irregular joints; (g) brecciated orebodies (Lobato et al., 2001a,c); (h) boudinaged oredodies in limb folds; (i) tear faults. The orebodies are related to the S2 mylonitic foliation generation subparallel to the host rocks compositional layering in the central portion of shear zones. The hydrothermal alteration associated is dominated by a chlorite-rich outer zone, an intermediate carbonate-rich zone and a white mica inner zone next to the ore (Vieira, 1991). Sulfidation and silicification commonly are related the two last alteration zones. A classification for the gold mineralization styles is presented by Lobato et al. (2001a,c), based on the proposal of Hodgson (1993): (a) stratabound, replacement deposits, generally in BIF; (b) disseminated deposits, related to hydrothermal alteration in shear zones; and (c) shear-related quartz–carbonate–sulfide veins, these cutting all host rocks.

Precise age of the gold mineralization was obtained for Morro Velho and Cuiabá deposits (Lobato et al., 2007-this volume). Hydrothermal monazite crystals yield U–Pb SHRIMP results of 2672 ± 14 Ma. Indirect constraints are suggested by the structural control of orebodies, implying a minimum Late Archean age as well (Zucchetti and Baltazar, 1998; Lobato et al., 2001a). Some Pb–Pb model ages were obtained for São Bento deposit (2650 Ma; DeWitt et al., 2000), Cuiabá deposit (2780 Ma–2670 Ma; Lobato et al., 2001c) and Bela Fama deposit (2710 Ma; Thorpe et al., 1984). Noce et al. (2007-this volume) present Pb and Sr isotopic data on sulfides and carbonates from the Cuiabá gold deposit (~2700 Ma). The geochronological data of the Quadrilátero Ferrífero are comprehensively discussed by Lobato et al. (2007-this volume) and Noce et al. (2007-this volume).

7. Discussion and conclusions

This paper develops a new proposal for the greenstone sequence subdivision in the QF. This proposal is based mainly in the sedimentary lithofacies associations defined by sedimentary facies analysis, supported by some petrographic results. The associations are summarized bellow:

- The mafic–ultramafic volcanic association contains the most primitive basalts and komatiites both formed from a mantle plume and similar to submarine plateau basalts. Arc-related and contaminated tholeiites are also present.
- The volcano–chemical–sedimentary lithofacies association is made up of arc-related tholeiites and tholeiites similar to submarine plateau basalts. Abundant BIF and ferruginous chert are intercalated. There is a transition between these two lithofacies associations.
- The clastic–chemical–sedimentary association represents deep-water sediments deposited in a pelagic environment.
- The volcaniclastic association is represented by four lithofacies, interpreted as sedimentary rocks of upper to middle-alluvial fans, fluvial systems and submarine turbidites. Felsic volcanic rocks are closely associated with the alluvial–fluvial lithofacies. The absence of shelf sediments suggests a rapid transition from a subaerial alluvial–fluvial environment to turbiditic deposits of submarine fans. This is typical of explosive volcanism producing emergent islands in an active tectonic environment, with erosion and rapid movement of pyroclastic material along the slopes of the volcanic cones (Ojakangas, 1985).
- The resedimented association is interpreted as turbidites having been deposited in at least three distinct environments: (1) the eastern graywackes (mixed and felsic sources) grade into pelagic sedimentary rocks; (2) northern graywackes (felsic source) are transitional with the volcaniclastic association graywackes, and (3) the southern carbonate-rich greywacke–argillite sequences (mixed and felsic sources) are transitional to tidal plain sandstone–siltstone lithofacies of the coastal association.
- The coastal association is restricted to sandstones with herringbone cross-bedding, ripple marks and large-scale cross-bedding, and to sandstone–siltstone lithofacies, with which the former are transitional.
- The non-marine association is made up of the clastic-continental alluvial–fluvial sedimentary rocks of the Casa Forte Formation (Maquiné Group), overlying in angular unconformity the Nova Lima Group in the central part of the QF.

7.1. Sedimentary cycles

This paper proposes the development of the sedimentary basins in four sedimentary cycles and related tectonic settings. The sedimentary cycle proposal is based on spatial correlation between the lithofacies associations, which are based on field relationships supported by petrographic features and chemical data.

Mafic–ultramafic volcanic and volcano–chemical–sedimentary lithofacies associations have been united in a unique sedimentary cycle, denominated Cycle 1. They are consistent with an extensional tectonic regimen of an oceanic basin spreading. They can be correlated to the 'Mafic Anorogenic Volcaniclastic–Orthochemical–Biogenic Association (MAVOB)' of Lowe (1994) and correspond to the 'THOLKOM-type assemblage' of Jackson et al. (1994).

Pelagic and chemical sediments of the clastic–chemical–sedimentary association are transitional to mixed source distal graywackes of the resedimented association. These two sedimentary sequences constitute the sedimentary Cycle 2. They could have been deposited during the final stages of the ocean basin extensional phase and onset of the subduction phase. The association is correlated to the 'Anorogenic Orthochemical Biogenic Association (AOB)' of Lowe (1994). Turbidites of the resedimented association in the eastern sector and associated pelagic sediments belong to the sedimentary Cycle 2. Southern carbonate-rich greywacke–argillite sequence along with the coastal association can be temporally correlated with the eastern sector sedimentary sequences and also attributed to the sedimentary Cycle 2.

Sandstone–siltstone lithofacies of the coastal association grades into carbonate-rich turbidites of the southern resedimented association. Based on similarity of their graywackes' REE patterns these sediments can be temporally correlated with the eastern sector sedimentary sequences and attributed to the sedimentary Cycle 2, despite of their different depositional and tectonic environments and metamorphic grade. The two sedimentary sequences describe a stable continental shelf environment. The local presence of conglomerate intercalated in turbidite reflects an environment of possible high energy related to local uplift because of subsequent extensional faults (Eriksson et al., 1994), next to continental margins. The set is equivalent to Lowe's (1994) 'Anorogenic Polycyclic Terrigenous Association (APT)'. The author states that, although shallow-water, quartz-rich, mature sandstones are not common in Archean greenstone belts, they develop locally, mainly in younger belts, post-3.0 Ga, as appears to be the case in the Rio das Velhas greenstone belt. Examples are described from the Chitradurga greenstone belt, India (Naqvi, 1986), in the Buhwa greenstone belt, Zimbabwe (Eriksson and Fedo, 1994) and in some belts of the Superior Province, Canada (Thurston and Chivers, 1990). They are interpreted as marginal deposits of ancient continental blocks or Archean micro-continents (Lowe, 1994).

Northern graywackes of the resedimented association are interpreted as submarine fan turbidites, which would have been deposited in a subduction phase, forming the sedimentary Cycle 3. They are similar to turbidite sequences (OTt) of Lowe's (1994) 'Orogenic Terrigenous Associations', interpreted as sediments related to an orogenic environment deposited within trenches, back-arc and fore-arc settings during the subduction. They are equivalent to the 'TURB-type assemblages' of Jackson et al. (1994).

The volcaniclastic association and related epiclastic turbidites also constitute the sedimentary Cycle 3. The volcanoclastic association is interpreted to be related to the formation of island arcs resulting from subduction related to the inversion during the orogenic phase of the oceanic basin. This lithofacies association and related epiclastic turbidites are equivalent to the 'Felsic/Intermediate Volcaniclastic–Terrigenous Association (FVT)' of Lowe (1994). They also correspond to the 'Central Volcanic Complexes' of Dimroth et al. (1983) and Hodgson and Hamilton (1989).

Coarse clastic, river-dominated sedimentary rocks of the non-marine association constitute the sedimentary Cycle 4. They are interpreted as deposits of the retroarc foreland-basin type, generated inside the basin and deformed during the second phase of the Archean compressive event (D2 structures). The Cycle 4 is correlated to the alluvial–fluvial sequences (OTaf) of Lowe's (1994) 'Orogenic Terrigenous Association' and the 'ALUFLU-type association' of Jackson et al. (1994).

7.2. Stratigraphic review

Despite of the scarcity of available geochronological data and the lack of techniques to determine the absolute age of sedimentary sequences, the relative stratigraphic positioning of these sequences is deduced. This paper proposes the following modifications to the formal stratigraphic subdivision of the greenstone sequence (Table 2):

- Cycles 1, 2 and 3 correspond respectively to lower, intermediary and upper units of the undivided Nova Lima Group. The Palmital Formation, basal of the Maquiné Group, is included in the Cycle 3, and therefore on the top of the Nova Lima Group. Cycle 4 represents the Casa Forte Formation, the superior unit of the Maquiné Group (Table 2). Fig. 15 summarises the tectonic environment of the sedimentary cycles and respective lithofacies associations.
- The sandstone–siltstone sequence of the central sector of the QF, the Palmital Formation of the Maquiné Group, has been interpreted as tidal plain

Table 2
Stratigraphic subdivision of the Rio das Velhas greenstone belt in the Quadrilátero Ferrífero

Rio das Velhas Supergroup	Greenschist facies	Amphibolite facies
Maquiné Group		
Cycle 4	–Non-marine association (Casa Forte Formation)	–
Unconformity		
Nova Lima Group		
Cycle 3	–Epiclastic proximal turbidites (Palmital Formation)	–
	–Epiclastic turbidites (Undivided)	–
	–Volcaniclastic association	–
Cycle 2	–Epiclastic distal turbidites	–Coastal association
	–Clastic–chemical–sedimentary association	–Carbonate-rich turbidites
Cycle 1	–Volcano–chemical–sedimentary association	–
	–Mafic–ultramafic volcanic association	–

deposits by Pedreira and Silva (1996) and Baltazar and Pedreira (1996, 1998). For this reason, Baltazar and Silva (1996) and Zucchetti et al. (1996, 1998) correlated it with the sandstones of Andaimes range, in the eastern sector of the QF and included it in the coastal association. However, the Palmital Formation is here considered as proximal turbidites (Atlas V. Corrêa Neto, personal communication, 2000) that are transitional to volcanogenic graywackes of the volcaniclastic association. They are interpreted as marine sediments proximal to volcanic edifices of an island arc environment. Dorr (1969) indicated a gradation between the Palmital Formation and the more phyllitic units of the Nova Lima Group, where there is only local unconformity between both units. Belo de Oliveira (1986) interpreted this unconformity as a thrust fault and, based on the gradation mentioned by Dorr (1969), suggested the removal of the Palmital Formation from the base of the Maquiné Group and its inclusion at the top of the Nova Lima Group. For the reasons above, and also considering that an important angular unconformity occurs at the contact of this formation with the overlying Casa Forte Formation, Belo de Oliveira's (1986)

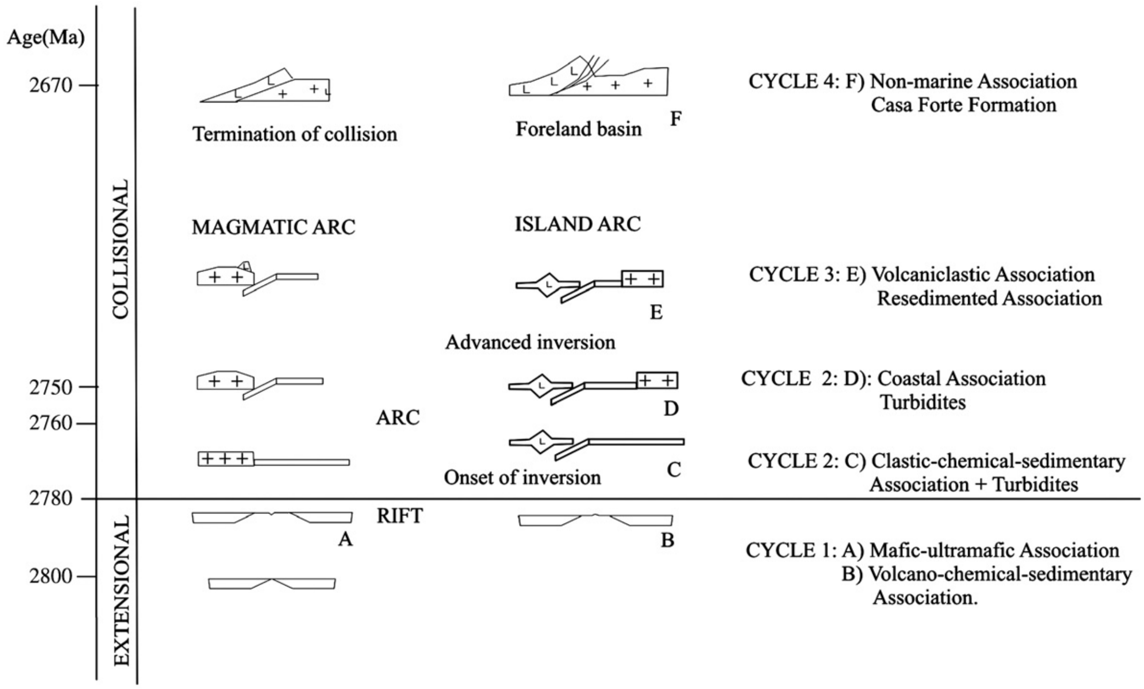

Fig. 15. Sketch of tectonic environment of sedimentary cycles and respective lithofacies associations (adapted from Jackson et al., 1994, Fig. 10).

proposition of including the Palmital Formation at the top of the Nova Lima Group appears most reasonable.

- Sedimentary Cycle 1 is the basal unit, deposited on an oceanic basin spreading. Radiometric dates were obtained from minor graywackes overlying komatiites. In the Carrapato deposit zircons yielded minimum ages between 2900 Ma and 3232 Ma (LA-ICPMS, Pb/Pb ages; Machado et al., 1996; Schrank and Machado, 1996b). In the Cuiabá deposit, detrital monazite yielded a concordant age at 2857±1 Ma (Schrank and Machado, 1996b; Schrank et al., 2002). These data show that the main sources for the Cycle 1 sediments are older than the last felsic volcanism, which has been dated at about 2780 Ma (Machado et al., 1992; Noce et al., 2002).
- Cycle 2 in the Santa Barbara block, was deposited in the final stages of basin extension, at the beginning of subduction and onset of felsic volcanism. In the São Bartolomeu block, Cycle 2 defines two distinctives tectono-sedimentary environments: (1) an initially stable continental shelf environment changing to (2) an unstable environment, in response to emplacement of plutons contemporaneous with felsic volcanism related to subduction, next to a continental block, in a possible magmatic arc environment. The U–Pb (detrital zircon-SHRIMP II) isotopic results from a quartz sandstone of the coastal association show a concordant minimum age of 2749±7 Ma (Suita et al., 2002). This represents the maximum age for this cycle and its deposition after the last felsic volcanism event (at 2780 Ma; Noce et al., 2002).
- Cycle 3 corresponds to an orogenic phase, during the inversion of the basin, related to the formation of island arcs and deposition of sediments in back-arc basins, during the subduction. At Morro Velho gold deposit, Schrank et al. (2002) obtained the 2799–2770 Ma age interval by U–Pb from detrital zircons of turbidites. A concordant age of 2705 Ma was obtained from detrital monazite (Schrank and Machado, 1996a).
- Cycle 4 is the upper unit and corresponds to the Casa Forte Formation, deposited in a retroarc foreland basin.

7.3. Structures and structural control on gold ores

Four generations of structures are recognized in the Rio das Velhas greenstone belt, related to three deformational events (Table 3). The first, Archean, in a fold-thrust style, with two generations of structures (D1 and D2), in a single progressive deformation, driven from N–NE to S–SW. D1 structures affected sedimentary cycles 1 to 3 and D2 structures affected also Cycle 4. D1 and D2 phases may be constrained between 2750 Ma and 2670 Ma. The second event (D3 structures) is attributed to diapiric uprising of batholiths, as metamorphic core complexes, related to a Transamazonian crustal extension (2100 to 1900 Ma). The final event (D4 structures) is a tangential compressional deformation, in a fold-thrust style, driven

Table 3
Synthesis of structural evolution of the Archean Rio das Velhas greenstone belt and Proterozoic cover sequences inside the Quadrilatero Ferrifero region

Age (Ma)	Tectonic event	Phase	Regime	Tectonic transport	Structures
2749–2670	Archean	D1	Compressive, simple shear	N to S	E-striking, S-verging thrust faults S-vergent tight to isoclinal folds, with ENE-plunging axes and open, flexural folds Axial–planar S1 foliation, subparallel to folded S_0 (355/65) Down-dip stretching and mineral lineation, intersection lineation (S_0 and S_1) parallel to fold axes
~2700	Archean	D2	Compressive, simple shear	NE to SW	NW-striking thrust faults (030–050/40–60) NW trending, SW-verging tight to isoclinal folds Axial–planar S_2 foliation (060/35-mylonitic foliation) Stretching lineation, mineral lineation (060–070/20–30)
2100–1900	Transamazonian	D3	Extension	WNW to ESE	Nucleation of regional synclines and onset of Minas Supergroup deposition Uplift of granite–gneissic basement as metamorphic core complexes Normal faults around the complexes
650–500	Brasiliano	D4	Compressive, simple shear	E to W	NS-striking, W-verging thrusts W-verging tight to isoclinal folds and open, normal folds Mylonitic and planar–axial S_4 foliation Stretching and mineral lineation plunging towards ESE

from the east to the west, attributed to the Brasiliano Orogenic Cycle (700 to 500 Ma).

Gold deposits are structurally controlled in the sense that hydrothermal fluids were channeled along deformation zones. The structural controls in the Rio das Velhas greenstone belt are as follows:

- On a regional scale, they are controlled by NW-striking and SW-vergent D2 shear zones, e.g., the São Vicente and Raposos faults (Fig. 14).
- On the deposit scale, the Au ores are confined to second- and third-order thrusts, related strike–slip faults and sheath folds.
- On the orebody scale, a wide variety of structures may be mineralized, including fault intersections, flexures and folds. In high-grade orebodies the preferential structures are cigar-shaped hinge folds ores and boudinaged and disrupted segments along S2 planes. Orebodies generally plunges subparallel to the NW-striking D2 thrusts. Where the D4 W-verging deformation is superimposed, ore plunges are modified by rotation/transposition around D4 fold axes.

7.4. Tectonic evolution

The evolutionary history of the Rio das Velhas greenstone belt is long and complex. This is corroborated by the following observations.

(1) The juxtaposition of (i) primitive high-Mg basalts and tholeiites, both similar to submarine plateaus originated from partial fusion of a mantle plume, (ii) arc-related tholeiites, and (iii) contaminated tholeiites.
(2) The occurrence of at least three volcanic episodes, at 3.03 Ga, at 2.93 Ga, and at 2.78 Ga, suggested by Noce et al. (2002), based on radiometric data from felsic volcanic rocks.
(3) The presence of turbidites older than 2.857 Ga (Schrank et al., 2002), deposited between the second and the third volcanic felsic activity.

The Rio das Velhas greenstone belt can be accounted as a collage of oceanic fragments, similar to the proposed model for the Abitibi greenstone belt by Desrochers et al. (1993). Noce et al. (2002) suggested that the greenstone belt can be a tectonic amalgamation of volcanic–sedimentary sequences generated in different tectonic environments. In the same way, Corfu and Andrews (1987) also described three distinct felsic volcanic episodes in the Red Lake greenstone belt, Canada.

The Rio das Velhas greenstone belt can be viewed as a structural collage of different terrains, represented by distinct tectonic settings. This is demonstrated by the spatial distribution of the sedimentary cycles controlled by shear zones, which juxtaposed tectonic blocks (Fig. 4) with distinct lithostructural characteristics and structural styles (Fig. 13).

Evidence for the presence of an older granite–gneissic terrain is indicated by 3560–3548 Ma U–Pb concordant ages on detrital zircons from turbidites of the Morro Velho gold deposit (Schrank et al., 2002); the 3198 Ma concordant age yielded by a detrital zircon from turbidites next to the town of Caeté (Schrank and Machado, 1996b); and 3809 Ma SHRIMP U–Pb age obtained in one detrital zircon from sandstones of the northern town of Itabirito (Suita et al., 2002). According to these authors, the Th/U ratio of this zircon is 0.9, which is common in magmatic zircon crystals from tonalites, suggesting contribution of an oldest continental crust. Thus, a greenstone belt evolution in at least two stages is envisaged:

(1) An Early Archean greenstone belt could have developed between 3030 Ma and 2930 Ma, age of the first and second volcanisms. It is represented by komatiites, primitive high-Mg basalts, tholeiites similar to submarine plateaus, and the older than 2857 Ma turbidites, deposited on a spreading ocean floor.
(2) A Late Archean greenstone belt related to the last felsic volcanism and represented by arc-related tholeiites and contaminated tholeiites. The Morro Velho-type turbidites (Schrank and Machado, 1996a), deposited in an arc-related environment and all essentially sedimentary lithofacies associations described are attributed to this stage.
(3) A major episode of magmatism and metamorphic activity, the Belo Horizonte Event (Schrank and Machado, 1996b; Schrank et al., 2002), occurred during the interval between the evolution of the early and late greenstone belts, marked by the 2920–2834 Ma age interval obtained by U–Pb from zircons in the TTG gneiss of the Bonfim and Belo Horizonte complexes.

The Late Archean greenstone belt evolution occurred between 2800 Ma and 2670 Ma as follows:

- 2800 to 2780 Ma: Extensional phase. Basalt lava flow in a spreading ocean floor. Deposition of Cycle 1 chemical sediments;
- 2780 to 2760 Ma: Onset of subduction phase. Felsic volcanism. Chemical and clastic sedimentation.

Morro Velho-type turbidites deposition. Onset of Cycle 2 deposition. Coeval granitic magmatic episode – the Rio das Velhas Event – at ca. 2780 to 2760 Ma, with the emplacement of granodioritic and tonalitic bodies in the Caeté and Bonfim complexes, respectively (Schrank and Machado, 1996b; Noce, 2000; Schrank et al., 2002);
- 2760 to 2750 Ma: Continued subduction phase. Cycle 2 coastal sandstone deposition in a stable continental margin away from the subduction zones and turbidite deposition next to subduction zones;
- 2750 to 2670 Ma: Advanced subduction phase and collision. Deposition of Cycle 3 volcaniclastic and epiclastic turbidites in trench and back-arc basins. Cycle 4 alluvial–fluvial deposition in a fore-arc basin, during the collision. Gold mineralization along D2 shear zones. Emplacement of granitic and granodioritic bodies in Bonfim and Belo Horizonte complexes (Machado and Carneiro, 1992; Machado et al., 1992; Chemale et al., 1994; Noce et al., 1998; Noce, 2000);
- 2600 to 2575 Ma: Emplacement of granitic and granodioritic bodies around the QF, representing the last episode of magmatism in the Late Archean (Romano, 1989; Romano et al., 1991; Endo, 1997; Noce et al., 1998; Noce, 2000).

The Proterozoic and Mesozoic covers evolution occurred as follows:

- 2580 to 2050 Ma: A crustal extension occurred in the interval with an initial rift phase and deposition of Minas Supergroup sediments in a passive continental margin (Renger et al., 1994).
- 2125 to 2000 Ma: Transamazonian orogeny. The QF area underwent an extensional tectonic with generation D3 structures, related to the uprising of batholiths as metamorphic core complexes. Isotopic remobilization in Archean rocks.
- 1750 to 1500 Ma: Mesoproterozoic rifting in the São Francisco Craton, with generation of the Espinhaço Supergroup basin and intrusion of mafic dikes (Chemale et al., 1994; Alkmim and Marshak, 1998).
- 1200 to 900 Ma: Crustal extension. Opening of Brasiliano/Pan-African proto-ocean (Chemale et al., 1994).
- 700 to 500 Ma: Brasiliano Orogeny. D4 structures generation in the QF, in a fold-thrust style, driven from east to west.
- <130 Ma: Mesozoic extensional tectonism with sedimentary basins opening and basic dikes intrusions (Chemale et al., 1994).

Acknowledgements

The authors acknowledge the Departamento Nacional da Produção Mineral (DNPM) for allowing the use of data pertaining to the Rio das Velhas Project, and the Geological Survey of Brazil (CPRM) for the support. Many people must be thanked for their support, discussions and/or access to unpublished data, including: A.V. Corrêa Neto, C.M. Noce, F.W.R. Vieira, J. Duchini Jr., L.C. Ribeiro-Rodrigues, L.M. Lobato, S. Martins Pereira. Colleagues at the Geological Survey of Brazil (CPRM) are acknowledged for cooperation. Special thanks are due to D.I. Groves and L.M. Lobato for carefully reviewing the manuscript, resulting in its significant improvement. We are indebted to F.J. Baars for the technical discussions and for having provided considerable assistance. M.L.C.R. Vasconcelos dispensed great help in putting together the reference list. M.F. Augusto, P.P. da Luz and V.C.A. Pereira drafted the figures, and C. Bacon translated the manuscript.

References

Alkmim, F.F., Marshak, S., 1998. Transamazonian orogeny in the Southern São Francisco Craton region, Minas Gerais, Brazil: evidence for Paleoproterozoic collision and collapse in Quadrilátero Ferrífero. Precambrian Research 90, 29–58.

Alkmim, F.F., Jordt-Evangelista, H., Marshak, S., Brueckner, H., 1994. Manifestações do evento Trans-Amazônico no Quadrilátero Ferrífero, MG. 38th Congresso Brasileiro de Geologia. Sociedade Brasileira de Geologia, Camboriú, pp. 75–76.

Allen, J.R.L., 1963. The classification of cross-stratified units with notes on their origin. Sedimentology 2, 93–114.

Allen, J.R.L., 1968. Current Ripples: their Relation to Patterns of Water and Sediment Motion. North-Holland Publishing Company, Amsterdam. 443 pp.

Almeida, F.F.M., 1967. Origem e evolução da plataforma brasileira. Departamento Nacional da Produção Mineral. Divisão Geologia Mineral, Boletim, vol. 241. Rio de Janeiro, Brasil, 36 pp.

Almeida, F.F.M., 1976. Estruturas do Pré-Cambriano inferior brasileiro. 29th Congresso Brasileiro de Geologia. Sociedade Brasileira de Geologia, Ouro Preto, pp. 201–202.

Almeida, F.F.M., Hasui, Y., 1984. O Pré-Cambriano do Brasil. Edgar Blücher, São Paulo. 378 pp.

Anders, E., Grevesse, N., 1989. Abundances of the elements: meteoritic and solar. Geochimica et Cosmochimica Acta 53, 197–214.

Arndt, N.T., Albarède, F., Nisbet, E.G., 1997. Mafic and ultramafic magmatism. In: de Witt, M.J., Ashwal, L.D. (Eds.), Greenstone Belts. Clarendon Press, Oxford, pp. 233–254.

Baltazar, O.F., 1996. Geologia estrutural. In: CPRM–Companhia de Pesquisa de Recursos Minerais. Projeto Rio das Velhas: Texto Explicativo do Mapa Geológico Integrado, escala 1:100.000. Departamento Nacional de Produção Mineral/CPRM–Serviço Geológico do Brasil, Belo Horizonte, p. 49–53.

Baltazar, O.F., 1998. Geologia estrutural. In: M. Zucchetti and O.F. Baltazar (Eds.), Projeto Rio das Velhas — Texto Explicativo do Mapa Geológico Integrado, escala 1:100.000. 2nd edition, Departamento Nacional de Produção Mineral/CPRM–Serviço Geológico do Brasil, Belo Horizonte, p. 49–53.

Baltazar, O.F., Silva, S.L., 1996. Projeto Rio das Velhas: Mapa Geológico Integrado do Supergrupo Rio das Velhas, escala 1:100.000. Departamento Nacional de Produção Mineral/ CPRM–Serviço Geológico do Brasil, Belo Horizonte.

Baltazar, O.F., Pedreira, A.J., 1996. Associações de litofácies. In: CPRM–Companhia de Pesquisa de Recursos Minerais. Projeto Rio das Velhas–Texto Explicativo do Mapa Geológico Integrado, escala 1:100.000. Departamento Nacional de Produção Mineral/ CPRM–Serviço Geológico do Brasil, Belo Horizonte, p. 43–48.

Baltazar, O.F., Pedreira, A.J., 1998. Associações litofaciológicas. In: M. Zucchetti and O.F. Baltazar (Eds.), Projeto Rio das Velhas–Texto Explicativo do Mapa Geológico Integrado, escala 1:100.000. 2nd edition, Departamento Nacional de Produção Mineral/CPRM–Serviço Geológico do Brasil, Belo Horizonte, p. 43–47.

Baltazar, O.F., Zucchetti, M., 2000. Rio das Velhas greenstone belt structural evolution, Quadrilátero Ferrífero, Minas Gerais, Brazil. 31th International Geological Congress. Rio de Janeiro, Brazil, CD-ROM.

Baltazar, O.F., Corrêa Neto, A.V., Silva, S.L., Zucchetti, M., Carvalho, J.B., Raposo, F.O., 1994. Uma tentativa preliminar de aplicação da estratigrafia de seqüências ao greenstone belt Rio das Velhas, Quadrilátero Ferrífero (MG). 38th Congresso Brasileiro de Geologia. Sociedade Brasileira de Geologia, Camboriú, pp. 82–83.

Baltazar, O.F., Rosière, C.A., Corrêa Neto, A.V., Silva, J.N., 1995. Geologia estrutural do Grupo Maquiné, Supergrupo Rio das Velhas, na porção central do Quadrilátero Ferrífero (MG). 5th Simpósio Nacional de Estudos Tectônicos. Sociedade Brasileira de Geologia, Gramado, pp. 11–13.

Belo de Oliveira, O.A., 1986. As falhas de empurrão e suas implicações na estratigrafia e metalogênese do Quadrilátero Ferrífero. 34th Congresso Brasileiro de Geologia. Sociedade Brasileira de Geologia, Goiânia, pp. 5–15.

Bouma, A.H., 1962. Sedimentology of Some Flysch Deposits. Elsevier, Amsterdam. 198 pp.

Butler, R.W.H., 1982. The terminology of structures in thrust belts. Journal of Structural Geology 4, 239–245.

Campbell, I.H., Griffiths, R.W., 1992. The changing nature of mantle hotspots through time: implications for the chemical evolution of the mantle. Journal of Geology 92, 497–523.

Campbell, I.H., Griffiths, R.W., Hill, R.E.T., 1989. Melting in an Archaean mantle plume: heads it's basalts, tails it's komatiites. Nature 339, 697–699.

Carneiro, M.A., 1992. O Complexo Metamórfico Bonfim Setentrional (Quadrilátero Ferrífero, MG): Litoestratigrafia e evolução geológica de um segmento de crosta continental do Arqueano. PhD thesis, Instituto de Geociências, Universidade de São Paulo. São Paulo, Brasil, 233 pp.

Chemale Jr., F., Rosière, C.A., Endo, I., 1991. Evolução tectônica do Quadrilátero Ferrífero, Minas Gerais: um modelo. Pesquisas 18 (2), 104–127.

Chemale Jr., F., Rosière, C.A., Endo, I., 1994. The tectonic evolution of the Quadrilátero Ferrífero, Minas Gerais, Brazil. Precambrian Research 65, 25–54.

Condie, K.C., 1994. Greenstone through time. In: Condie, K.C. (Ed.), Archean Crustal Evolution. Elsevier, Amsterdam, pp. 85–120.

Corfu, F., Andrews, A.J., 1987. Geochronological constraints on the timing of magmatism, deformation, and gold mineralization in the Red Lake greenstone belt, northwestern Ontario. Canadian Journal of Earth Sciences 24, 1302–1320.

Corrêa Neto, A.V., Baltazar, O.F., 1995. Compartimentação estrutural do greenstone belt Rio das Velhas no interior do Quadrilátero Ferrífero (MG). 5th Simpósio Nacional de Estudos Tectônicos. Sociedade Brasileira de Geologia, Gramado, pp. 15–17.

Corrêa Neto, A.V., Baltazar, O.F., Silva, S.L., 1994. Evolução estrutural do setor setentrional do greenstone belt Rio das Velhas (MG). 38th Congresso Brasileiro de Geologia. Sociedade Brasileira de Geologia, Camboriú, pp. 69–70.

Desrochers, J.P., Hubert, C., Ludden, J.N., Pilote, P., 1993. Accretion of Archean oceanic plateau fragments in the Abitibi greenstone belt, Canada. Geology 21, 451–454.

DeWitt, E., Thorman, C.H., Ladeira, E., Zartman, R.E., Landis, G.P., Wooden, J.L., 2000. Origin and age of gold deposits at São Bento and Morro Velho, Brazil. 31th International Geological Congress, Rio de Janeiro, Brazil, CD-ROM.

Dimroth, E., Imreh, L., Goulet, N., Rocheleau, M., 1983. Evolution of the south-central segment of the Archean Abitibi Belt, Quebec: Part III. Plutonic and metamorphic evolution and geotectonic model. Canadian Journal of Earth Sciences 20, 1374–1388.

Dorr II, J.V., 1969. Physiographic, stratigraphic and structural development of the Quadrilátero Ferrífero, Minas Gerais, Brazil. United States Geological Survey Professional Paper 614-A. 110 pp.

Dorr II, J.V., Gair, J.E., Pomerene, J.B., Rynearson, G.A., 1957. Revisão da estratigrafia pré-cambriana do Quadrilátero Ferrífero, Brasil. Departamento Nacional da Produção Mineral, Divisão de Fomento da Produção Mineral, Avulso, vol. 81. 31 pp.

Einsele, G., 1992. Sedimentary Basins; Evolution, Facies and Sediment Budget. Springer-Verlag, Berlin. 628 pp.

Endo, I., 1997. Regimes tectônicos do Arqueano e Proterozóico no interior da placa sanfranciscana: Quadrilátero Ferrífero e áreas adjacentes, Minas Gerais. PhD thesis, Instituto Geociências, Universidade de São Paulo. São Paulo, Brasil, 2 volumes, 243 pp.

Endo, I., Fonseca, M.A., 1992. Sistema de cisalhamento Fundão–Cambotas no Quadrilátero Ferrífero–MG: geometria e cinemática. 6th Simpósio de Geologia de Minas Gerais. Sociedade Brasileira de Geologia, Ouro Preto. Revista da Escola de Minas 45 (1/2), pp. 28–31.

Endo, I., Nalini Jr., H.A., 1992. Geometria e cinemática das estruturas extensionais e compressionais na borda oeste do sinclinal Moeda, QF. 6th Simpósio de Geologia de Minas Gerais. Sociedade Brasileira de Geologia, Ouro Preto, Revista da Escola de Minas 45 (1/2), pp. 15–17.

Eriksson, K.A., Fedo, C.M., 1994. Archean synrift and stable-shelf sedimentary successions. In: Condie, K.C. (Ed.), Archean Crustal Evolution. Elsevier, Amsterdam, pp. 171–204.

Eriksson, K.A., Krapez, B., Fralick, P.W., 1994. Sedimentology of Archean greenstone belts: signatures of tectonic evolution. Earth-Science Reviews 37, 1–88.

Féboli, W.L., Signorelli, N., 1996. Sinopse Geológica da Folha Itabirito: Projeto Rio das Velhas. Departamento Nacional da Produção Mineral/Companhia de Pesquisa de Recursos Minerais, Belo Horizonte, pp. 34–43.

Gair, J.E., 1962. Geology and ore deposit of the Nova Lima and Rio Acima quadrangles, Minas Gerais, Brazil. United States Geological Survey Professional Paper 341-A. 67 pp.

Golia, A., 1997. Petrografia e geoquímica dos metassedimentos do Grupo Nova Lima, greenstone belt Rio das Velhas na região de São Bartolomeu: modelagem de área-fonte, proveniência e ambiente tectônico. MSc thesis, Departamento de Geologia da Escola de Minas, Universidade Federal de Ouro Preto. Ouro Preto, Brasil, 142 pp.

Herz, N., 1970. Gneissic and igneous rocks of the Quadrilátero Ferrífero, Minas Gerais, Brazil. United States Geological Survey Professional Paper 641-B. 58 pp.

Herz, N., 1978. Metamorphic rocks of the Quadrilátero Ferrífero, Minas Gerais, Brazil. United States Geological Survey Professional Paper 641-C. 81 pp.

Hodgson, C.J., 1993. Mesothermal lode-gold deposits. In: Kirkham, R.V., Sinclair, W.D., Thorpe, R.I., Duke, J.M. (Eds.), Mineral Deposit Modeling. Geological Association of Canada Special Paper, vol. 28, pp. 635–678.

Hodgson, C.J., Hamilton, J.V., 1989. Gold mineralization in the Abitibi greenstone belt: end stage of Archean collisional tectonics? Economic Geology Monograph 6, 86–100.

Jackson, S.L., Fyon, J.A., Corfu, F., 1994. Review of Archean supracrustal assemblages of the southern Abitibi greenstone belt in Ontario, Canada: products of microplate interaction within a large-scale plate-tectonic setting. Precambrian Research 65, 183–205.

Ladeira, E.A., 1980. Metalogenesis of gold at the Morro Velho mine, and in the Nova Lima District, Quadrilátero Ferrífero, Minas Gerais, Brazil. PhD thesis, Department of Geology, University of Western Ontario. London, Canada, 272 pp.

Ladeira, E.A., Viveiros, J.F.M., 1984. Hipótese sobre a estruturação do Quadrilátero Ferrífero com base nos dados disponíveis. Sociedade Brasileira de Geologia, Boletim Especial 4, Belo Horizonte, pp. 1–14.

Ladeira, E.A., Roeser, H.M.P., Tobschal, H.J., 1983. Evolução petrogenética do Cinturão de Rochas Verdes, Rio das Velhas, Quadrilátero Ferrífero, Minas Gerais. 2th Simpósio de Geologia de Minas Gerais. Sociedade Brasileira de Geologia, Belo Horizonte, pp. 149–165.

Lobato, L.M., Ribeiro-Rodrigues, L.C., Vieira, F.W.R., 2001a. Brazil's premier gold province: Part II. Geology and genesis of gold deposits in the Archean Rio das Velhas greenstone belt, Quadrilátero Ferrífero. Mineralium Deposita 36, 249–277.

Lobato, L.M., Ribeiro-Rodrigues, L.C., Zucchetti, M., Noce, C.M., Baltazar, O.F., Silva, L.C., Pinto, C.P., 2001b. Brazil's premier gold province: Part I. The tectonic, magmatic, and structural setting of the Archean Rio das Velhas greenstone belt, Quadrilátero Ferrífero. Mineralium Deposita 36, 228–248.

Lobato, L.M., Ribeiro-Rodrigues, L.C., Costa, M.N.S., Martins, R., Lehne, E., Alves, J.V., Tassinari, C.C.G., Vieira, F.W.R., Biasi, E.E., Silva, R.C.F., Pereira, V.C.A., Noce, C.M., 2001c. Depósito de ouro Cuiabá, Quadrilátero Ferrífero, Minas Gerais. In: H. Jost, J.A. Brod, E.T. Queiroz (Coordinators), Caracterização de Depósitos Auríferos em Distritos Mineiros Brasileiros. Departamento Nacioanl da Produção Mineral/Agência para o Desenvolvimento Tecnológico da Indústria Mineral Brasileira, Brasília, p. 3–77.

Lobato, L.M., Santos, J.O.S., McNaughton, N.J., Fletcher, I.R., Noce, C.M., 2007. U-Pb SHRIMP monazite ages of the giant Morro Velho and Cuiabá gold deposits, Rio das Velhas greenstone belt, Quadrilátero Ferrífero, Minas Gerais, Brazil. Ore Geology Reviews 32, 674–680 (this volume). doi:10.1016/j.oregeorev.2006.11.007.

Loczy, L., Ladeira, E.A., 1976. Geologia Estrutural e Introdução à Geotectônica. Edgar Blücher, São Paulo. 528 pp.

Lowe, D.R., 1994. Archean greenstone-related sedimentary rocks. In: Condie, K.C. (Ed.), Archean Crustal Evolution. Elsevier, Amsterdam, pp. 121–169.

Machado, N., Carneiro, M.A., 1992. U–Pb evidence of late Archean tectono-thermal activity in the southern São Francisco shield, Brazil. Canadian Journal of Earth Science 29, 2341–2346.

Machado, N., Noce, C.M., Ladeira, E.A., Belo de Oliveira, O., 1992. U–Pb geochronology of Archean magmatism and Proterozoic metamorphism in the Quadrilátero Ferrífero, southern São Francisco Craton, Brazil. Geological Society American Bulletin 104, 1221–1227.

Machado, N., Schrank, A., Noce, C.M., Gauthier, G., 1996. Ages of detrital zircon from Archean–Paleoproterozoic sequences: implications for greenstone belt setting and evolution of a Transamazonian foreland basin in Quadrilátero Ferrífero, southeast Brazil. Earth and Planetary Science Letters 141, 259–276.

Machado, N., Schrank, A., Abreu, F.R., Knauer, L.G., Almeida-Abreu, P.A., 1989. Resultados preliminares da geocronologia U–Pb na Serra do Espinhaço Meridional. 15th Simpósio de Geologia de Minas Gerais. Sociedade Brasileira de Geologia, Belo Horizonte, pp. 171–174.

Malouf, R.F., Corrêa Neto, A.V., 1996. O Supergrupo Rio das Velhas na Folha Conceição do Rio Acima: Projeto Rio das Velhas. Departamento Nacional da Produção Mineral/Companhia de Pesquisa de Recursos Minerais, Belo Horizonte, pp. 17–23.

Marshak, S., Alkmim, F.F., 1989. Proterozoic contraction/extension tectonics of the southern São Francisco region, Minas Gerais, Brazil. Tectonics 8, 555–571.

Marshak, S., Alkmim, F.F., Jordt-Evangelista, H., 1992. Proterozoic crustal extension and the generation of dome-and-keel structure in an Archean granite–greenstone terrane. Nature 357, 491–493.

Marshak, S., Alkmim, F.F., Jordt-Evangelista, H., Brueckner, H.K., 1993. Aspects of the Precambrian tectonic evolution of the southern São Francisco craton and its eastern margin, Brazil. Geological Society of America, Abstracts with Programs 25, 298–299.

Marshak, S., Tinkhan, M.D., Alkmim, F.F., Brueckner, H.K., Bornhorst, T., 1997. Dome-and-keel provinces formed during Paleoproterozoic origenic collapse — core complexes, diapirs, or neither? Examples from Quadrilátero Ferrífero (Brazil) and the Penokean Orogen (USA). Geology 25, 415–418.

Martins Pereira, S.L., Lobato, L.M., Ferreira, J.E., Jardim, E.C., 2007. Nature and origin of the BIF-hosted São Bento gold deposit, Quadrilátero Ferrífero, Brazil, with special emphasis on structural controls. Ore Geology Reviews 32, 571–595 (this volume).

McLennan, S.M., Taylor, S.R., 1991. Sedimentary rocks and crustal evolution: tectonic setting and secular trends. Journal of Geology 99, 1–21.

Mueller, W., Chown, E.H., Sharma, K.N.M., Tait, L., Rocheleau, M., 1989. Paleogeographic and paleotectonic evolution of a basement-controlled Archean supracrustal sequence, Chibogamau–Caopatina, Quebec. Journal of Geology 97, 399–420.

Mutti, E., 1992. Turbidite Sandstones. S. Donato Milanese, Agip S.P.A. 275 pp.

Naqvi, S.M., 1986. Geochemical characters and tectonic evolution of the Chitradurga Schist Belt: an Archean suture (?) of the Dharwar Craton, India. In: de Witt, M.J., Ashwal, L.D. (Eds.), Workshop on Tectonic Evolution of Greenstone Belts. Lunar and Planetary Institute Technical Report, vol. 86–10, pp. 160–161.

Noce, C.M., 2000. Geochronology of the Quadrilátero Ferrífero: a review. Geonomos 8 (1), 15–23.

Noce, C.M., Machado, N., Teixeira, W., 1994. O complexo Belo Horizonte e a evolução arqueana do Quadrilátero Ferrífero, Minas Gerais. 38th Congresso Brasileiro de Geologia. Sociedade Brasileira de Geologia, Camboriú, pp. 68–69.

Noce, C.M., Machado, N., Teixeira, W., 1998. U–Pb geochronology of gneisses and granitoids in the Quadrilátero Ferrífero (southern São Francisco craton): age constraints for Archean and Paleoproterozoic magmatism and metamorphism. Revista Brasileira de Geociências 28, 95–102.

Noce, C.M., Dantas, E.L., Lobato, L.M., Zucchetti, M., Baltazar, O.F., 2002. Múltiplos eventos de vulcanismo no greenstone belt Rio das

Velhas, Quadrilátero Ferrífero (MG): novos dados U–Pb, implicações geotectônicas e metalogenéticas. 41th Congresso Brasileiro de Geologia. Sociedade Brasileira de Geologia, João Pessoa, p. 522.

Noce, C.M., Tassinari, C.G., Lobato, L.M., 2007. Geochronological framework of the Quadrilátero Ferrífero, with emphasis on the age of gold mineralization hosted in Archean greenstone belts. Ore Geology Reviews 32, 500–510 (this volume). doi:10.1016/j.oregeorev.2005.03.019.

Ojakangas, R.W., 1985. Review of Archean clastic sedimentation, Canadian Shield: major felsic volcanic contributions to turbidite and alluvial fan-fluvial facies associations. In: Ayres, L.D., Thurston, P.C., Card, K.D., Weber, W. (Eds.), Evolution of Archean Supracrustal Sequences. Geological Association of Canada Special Paper, vol. 28, pp. 23–47.

Oliveira, A.H., Guitarrari, M.M., Achôa, A.B., Costa, M.P., Carneiro, M.A., Fonseca, M.A., 1997. Tectônica compressiva (NE–SW) nas rochas do Supergrupo Rio das Velhas, borda NW do Complexo Metamórfico Bação, QF, MG. 9th Simpósio de Geologia de Minas Gerais. Sociedade Brasileira de Geologia, Belo Horizonte, Boletim, vol. 14, pp. 70–71.

O'Rourke, J.E., 1957. The stratigraphy of metamorphic rocks of the Rio de Pedras and Gandarela quadrangles, Minas Gerais, Brazil. PhD thesis, University of Winscosin. Winscosin, 106 pp.

Pedreira, A.J., Silva, S.L., 1996. Sistemas deposicionais do greenstone belt Rio das Velhas, Quadrilátero Ferrífero, Minas Gerais. 39th Congresso Brasileiro de Geologia. Sociedade Brasileira de Geologia, Salvador, pp. 138–140.

Polat, A., Kerrich, R., 2000. Archean greenstone belt magmatism and the continental growth-mantle evolution connection: constraints from Th–U–Nb-LREE systematics of the 2.7 Ga Wawa subprovince, Superior Province, Canada. Earth and Planetary Science Letters 175, 41–54.

Renger, F.S., Noce, C.M., Romano, A.W., Machado, N., 1994. Evolução sedimentar do Supergrupo Minas: 500 Ma de registro geológico no Quadrilátero Ferrífero, Minas Gerais, Brasil. Geonomos 2, 1–11.

Ribeiro-Rodrigues, L.C., 1998. Gold in Archaean banded iron-formation of the Quadrilátero Ferrífero, Minas Gerais, Brazil — the Cuiabá mine. PhD thesis, Aachen University of Technology. Aachen, Germany, 264 pp.

Rodrigues, F.A.C., Costa, A.F., Souza, R.A.C., Rosière, C.A., 1989. Sistemas de cavalgamento do nordeste do Quadrilátero Ferrífero. 5th Simpósio de Geologia de Minas Gerais. Sociedade Brasileira de Geologia, Belo Horizonte, Boletim, vol. 10, pp. 6–10.

Romano, A.W., 1989. Evolution tectonique de la région MW du Quadrilatère Ferrifère-Minas Gerais. Brésil. PhD thesis, Université de Nancy I. Nancy, France, 259 pp.

Romano, A.W., Bertrand, J.M., Michard, A., Zimmermann, J.L., 1991. Tectonique tangentielle et décrochements d'âge Protérozoïque inférier (orogenése transamazonienne, environ 2000 Ma) au Nord du "Quadrilatére Ferrifére" (Minas Gerais, Brésil). Comptes Rendus de l'Académie des Sciences de Paris 313, 1195–1200.

Rynearson, G.A., Pomerene, J.B., Dorr II, J.V., 1954. Contato basal da Série Minas na parte ocidental do Quadrilátero Ferrífero, Minas Gerais Brasil. Departamento Nacional da Produção Mineral, Divisão de Geologia e Mineralogia, Rio de Janeiro, Avulso, vol. 34, pp. 1–18.

Sales, M., 1998. The geological setting of the Lamego iron-formation-hosted gold deposits, Quadrilátero Ferrífero district, Minas Gerais, Brazil. MSc thesis, Queen's University. Kingston, Ontario, Canada, 182 pp.

Sandeman, H.A., Hanmer, S., Davis, W.J., Ryan, J.J., Peterson, T.D., 2004. Neoarchaean volcanic rocks, Central Hearne supracrustal belt, Western Churchill Province, Canada: geochemical and isotopic evidence supporting intra-oceanic, supra-subduction zone extension. Precambrian Research 134, 113–141.

Schorscher, H.D., 1976. Polimetamorfismo do Pré-Cambriano na região de Itabira, Minas Gerais. 29th Congresso Brasileiro de Geologia. Sociedade Brasileira de Geologia, Ouro Preto, pp. 194–195.

Schorscher, H.D., 1978. Komatiítos na estrutura "Greenstone Belt" Série Rio das Velhas, Quadrilátero Ferrífero, Minas Gerais, Brasil. 30th Congresso Brasileiro de Geologia. Sociedade Brasileira de Geologia, Recife, pp. 292–293.

Schorscher, H.D., 1979. Evolução geotectônica e petrogenética do embasamento arqueano do Quadrilátero Ferrífero. Anais da Academia Brasileira de Ciéncias 51, 767–768.

Schrank, A., Machado, N., 1996a. Idades U–Pb em monazitas e zircões das minas de Morro Velho e Passagem de Mariana–Quadrilátero Ferrífero (MG). 39th Congresso Brasileiro de Geologia. Sociedade Brasileira de Geologia, Salvador, pp. 470–472.

Schrank, A., Machado, N., 1996b. Idades U–Pb em monazitas e zircões do distrito aurífero de Caeté, da mina de Cuiabá e do depósito de Carrapato–Quadrilátero Ferrífero (MG). 39th Congresso Brasileiro de Geologia. Sociedade Brasileira de Geologia, Salvador, pp. 473–475.

Schrank, A., Machado, N., Stern, R., 2002. Eventos no Arqueano com base em idades U/Pb–SHRIMP de zircões detríticos em metassedimentos da mina de Morro Velho–Quadrilátero Ferrífero–Minas Gerais. 41th Congresso Brasileiro de Geologia. Sociedade Brasileira de Geologia, João Pessoa, p. 527.

Selley, R.C., 1988. Applied Sedimentology. Academic Press, London. 446 pp.

Sichel, S.E., 1983. Geologia das rochas Pré-Cambrianas da região de Barão de Cocais e geoquímica preliminar dos komatiítos do Supergrupo Rio das Velhas, Quadrilátero Ferrífero, MG. MSc thesis, Departamento de Geologia, Universidade Federal do Rio de Janeiro. Rio de Janeiro, Brasil, 232 pp.

Silva, L.C., 1996. Petrologia e litogeoquímica. In: Companha de Pesquisa de Recursos Minerais. Projeto Rio das Velhas–Texto Explicativo do Mapa Geológico Integrado, escala 1:100.000. Departamento Nacional de Produção Mineral/CPRM–Serviço Geológico do Brasil, Belo Horizonte, 55–104.

Silva, L.C., 1998. Petrologia e litogeoquímica. In: M. Zucchetti, O.F. Baltazar (Eds.), Projeto Rio das Velhas–Texto explicativo do mapa geológico integrado, escala 1:100.000. 2nd ed., Departamento Nacional de Produção Mineral/CPRM–Serviço Geológico do Brasil, Belo Horizonte, 55–103.

Silva, L.C., Noce, C.M., Lobato, L.M., 2000. Dacitic volcanism in the course of the Rio das Velhas (2800–2960 Ma) Orogeny: a Brazilian Archean analogue (TTD) to the modern adakites. Revista Brasileira de Geociências 30, 384–387.

Suita, M.T.F., Hartmann, L.A., Endo, I., Santos, J.O.S., McNaughton, N.J., 2002. The oldest detrital zircon in South America — 3.8 Ga, determined by SHRIMP geochronology from a Quadrilátero Ferrífero sandstone. 41th Congresso Brasileiro de Geologia. Belo Horizonte, João Pessoa, p. 528.

Sun, S.S., McDonough, W.F., 1989. Chemical and isotopic systematics of oceanic basalts: implications for mantle composition and processes. In: Saunders, A.D., Norry, M.J. (Eds.), Magmatism in Ocean Basins. Geologocal Society of London Special Publication, vol. 42, pp. 313–345.

Sylvester, P.L., Harper, G.D., Byerly, G.R., Thurston, P.C., 1997. Volcanic aspects. In: de Witt, M.J., Ashwal, L.D. (Eds.), Greenstone Belts. Clarendon Press, Oxford, pp. 55–90.

Taylor, S.R., McLennan, S.M., 1985. The Continental Crust: its Composition and Evolution. Blackwell Scientific Publications, Oxford. 312 pp.

Teixeira, W., 1985. A evolução geotectônica da porção meridional do Cráton do São Francisco, com base em interpretações geocronológicas. PhD thesis, Instituto Geociências, Universidade de São Paulo. São Paulo, Brasil, 207 pp.

Teixeira, W., Carneiro, M.A., Noce, C.M., Machado, N., Sato, K., Taylor, P.N., 1996. Pb, Sr and Nd isotope constraints on the Archean evolution of gneissic–granitoid complexes in the southern São Francisco craton, Brazil. Precambrian Research 78, 151–164.

Thorpe, R.I., Cumming, G.L., Krstic, D., 1984. Lead isotope evidence regarding age of gold deposits in the Nova Lima district, Minas Gerais, Brazil. Revista Brasileira de Geociências 14, 147–152.

Thurston, P.C., Chivers, K.M., 1990. Secular variation in greenstone sequence development emphasizing Superior Province, Canada. Precambrian Research 46, 21–58.

Tucker, M.E., 1996. Sedimentary Rocks in the Field, 2nd edition. John Wiley and Sons, Chichester. 153 pp.

Vial, D.S., 1988. Mina de ouro de Cuiabá, Quadrilátero Ferrífero, Minas Gerais. In: Schobbenhaus, C., Coelho, C.E.S. (Eds.), Metais básicos não ferrosos, ouro e alumínio. Principais Depósitos Minerais do Brasil 3. Departamento Nacional de Produção Mineral/Companhia Vale do Rio Doce, Brasília, Brasil, pp. 413–419.

Vial, D.S., DeWitt, E., Lobato, L.M., Thorman, C.H., 2007. The geology of the Morro Velho gold deposit in the Archean Rio das Velhas greenstone belt, Quadrilátero Ferrífero, Brazil. Ore Geology Reviews 32, 511–542 (this volume).

Vieira, F.W.R., 1991. Textures and processes of hydrothermal alteration and mineralization in the Nova Lima Group, Minas Gerais, Brazil. In: Ladeira, E.A. (Ed.), Proceedings of Brazil Gold '91. A.A. Balkema, Rotterdam, pp. 319–325.

Vieira, F.W.R., 1992. Geologia da mina de Cuiabá, níveis 03 e 04. Technical report, Mineração Morro Velho S. A. Nova Lima, Brasil, 23 pp.

Zucchetti, M., 1998. Geoquímica dos metabasaltos do Grupo Nova Lima, Supergrupo Rio das Velhas, Quadrilátero Ferrífero, Minas Gerais. MSc thesis, Instituto Geociências, Universidade Federal de Minas Gerais. Belo Horizonte, Brasil, 124 pp.

Zucchetti, M., Baltazar, O.F. (Eds.), 1998. Projeto Rio das Velhas–Texto explicativo do mapa geológico integrado, escala 1:100,000. 2nd ed. Departamento Nacional da Produção Mineral/CPRM–Serviço Geológico do Brasil, Belo Horizonte, Brazil, 121 pp.

Zucchetti, M., Baltazar, O.F., 2000. Rio das Velhas Greenstone Belt lithofacies associations, Quadrilátero Ferrífero, Minas Gerais, Brazil. 31th International Geological Congress, Rio de Janeiro, Brazil, CD-ROM.

Zucchetti, M., Baltazar, O.F., Raposo, F.O., 1996. Estratigrafia. In: Companhia de Pesquisa de Recursos Minerais. Projeto Rio das Velhas–Texto Explicativo do Mapa Geológico Integrado, escala 1:100.000. Departamento Nacional de Produção Mineral/CPRM–Serviço Geológico do Brasil, Belo Horizonte, p. 13–42.

Zucchetti, M., Baltazar, O.F., Raposo, F.O., 1998. Estratigrafia. In: M. Zucchetti, O.F. Baltazar (Eds.), Projeto Rio das Velhas–Texto explicativo do mapa geológico integrado, escala 1:100.000. 2nd ed. Departamento Nacional de Produção Mineral/CPRM–Serviço Geológico do Brasil, Belo Horizonte, p. 13–42.

Zucchetti, M., Lobato, L.M., Baltazar, O.F., 2000a. Volcanic and volcaniclastic features in Archean rocks and their tectonic environment, Rio das Velhas Greenstone Belt, Quadrilátero Ferrífero, MG. Brazil. Revista Brasileira de Geociências 30, 388–392.

Zucchetti, M., Lobato, L.M., Baars, F.J., 2000b. Genetically diverse basalt geochemical signatures developed in the Rio das Velhas Greenstone Belt, Quadrilátero Ferrífero, Minas Gerais, Brazil. Revista Brasileira de Geociências 30, 397–402.